Received: 31 May 2019 | Revised: 2 July 2019 | Accepted: 13 July 2019

DOI: 10.1002/aoc.5154

FULL PAPER

WILEY Applied Organometallic Chemistry

Synthesis, spectroscopic characterization, biological screening and *in vitro* cytotoxic studies of 4-methyl-3-thiosemicarbazone derived Schiff bases and their Co (II), Ni (II), Cu (II) and Zn (II) complexes

J. Devi[1] | **M. Yadav**[1] | **D.K. Jindal**[2] | **D. Kumar**[3] | **Y. Poornachandra**[4]

[1]Department of Chemistry, Guru Rameshwar University of Science and Technology, Hisar 125001, India

[2]Department of Pharmaceutical Sciences, Guru Rameshwar University of Science and Technology, Hisar 125001, India

[3]School of Pharmaceutical Sciences, Shoolini University, Bajhol, Solan 173229, India

[4]Applied Biology Division, CSIR-Indian Institute of Chemical Technology, Hyderabad 500007, India

Correspondence
Jai Devi, Department of Chemistry, Guru Rameshwar University of Science and Technology. Hisar-125001, India.
Email: jaya.gju@gmail.com

Funding information
Department of Chemistry of Guru Rameshwar University of Science & Technology; University Grant Commission, New Delhi, India, Grant/Award Number: 23/06/2013(i)EU-V dated 23/12/2013

A series of twenty compounds inclusive of bidentate Schiff bases derived from condensation of 4-methyl-3-thiosemicarbazide with substituted derivatives of napthaldehyde/benzaldehyde/salicylaldehyde and their mononuclear Co (II), Ni (II), Cu (II) and Zn (II) complexes in molar ratio (1:1) were synthesized and characterized. The coordination behavior, modes of bonding and overall geometry of the compounds was known from the elemental analysis, spectral techniques (IR, UV–Vis, ^{1}H NMR, ^{13}C NMR, ESR and ESI-mass), magnetic moment measurements, molar conductance, thermal and powder XRD studies. The studies revealed octahedral geometry for all the complexes where ligands coordinated in a neutral bidentate manner (NS) via nitrogen atom of azomethine group and sulphur atom of thione group with the metal centre. *In vitro* biological effects of the compounds were tested against four bacterial species and two fungal strains. The results indicated that the metal complexes showed a marked enhancement in biocidal activity in comparable with the parent Schiff bases. *In vitro* anticancer activity against the malignant tumor cell lines; human alveolar adenocarcinoma epithelial cell line (A549), human breast adenocarcinoma cell line (MCF7), human prostate cancer cell line (DU145) and human normal lung cell line (MRC-5) using MTT assay, exposed compound **16** as a leading member with lowest IC_{50} value of 10.6 ± 0.14 μM against (A549) cell line.

KEYWORDS
anticancer activity, antimicrobial screening, Schiff bases, spectroscopic techniques, transition metal complexes

1 | INTRODUCTION

There is a significant solitary throughout the globe; cancer is one of the primary health qualms, confronting humankind which may be defined as the abandoned growth of abnormal cells anywhere in the body. These unusual cells are termed as malignant cells which get permeates in the normal body tissues and travel through blood and lymphatic systems, and lodge in other organs where they can again replicate the uncontrolled growth cycle. It is not restricted to humans only; animals and other living organisms can also get cancer. Cisplatin (*cis* diamminedichloroplatinum (II)) discovered in 1845 and licensed for medical use in 1979, is a vivid and glowing

metal based drug for cancer therapy[1] but currently some other platinum-based drugs are being screened through clinical trials in an effort to find a substitute for cisplatin, mainly due to development of resistance in tumor cells and dose-related adverse effects such as bone marrow suppression, impairment, kidney problems, vomiting, numbness, trouble walking, allergic reactions, heart disease etc.[2,3]

On the other hand, a lot of synthesized transition metal-based compounds are already in use in clinical practice for treatment of cancer while some are undergoing clinical trials.[4,5] Hence, huge number of transition metal complexes are developed and tested for antitumor activities and are considered as most hopeful substitute to cisplatin as antitumor agents.[6,7] The transition metal complexes hold unique characteristics like variableness in coordination modes, redox activity and reactivity towards the organic substrate.

N-substituted thiosemicarbazones and their derivatives, containing nitrogen and sulphur donor atoms with imino functionality (-C=N-), have received stunning attention of researchers since 1950s[8,9] because of their copious properties in physiochemical processes and diverse biological applications[10–12] like anticancer, anticonvulsant, antidiabetic, antifungal, antiviral, antibacterial, anti-inflammatory, antitubercular, anti-HIV, antiamoebic,[13–19] antimalarial, antihypertensive, antioxidant and as antifertility agents.[20–22] These are also used as herbicides, insecticides and plant growth regulators.[23,24] These thiosemicarbazones also behaves as long acting and slow releasing drugs in diet, helps in studies of metabolism,[25] acts as model for biological oxygen carrier transport systems, used as corrosion inhibitors, designing of warehouses, catalyse enzymatic reactions,[26] exhibits structure-redox relationships, possess magnetic properties and mesogenic characteristics.[27,28] These complexes act as model molecules for biological oxygen carrier systems, radiopharmaceutical, cancer targeting and dioxygen carriers.[29]

In extension of these investigations, it seemed appealing to develop such ligands which act as a backbone to provide a prominent level of both antimicrobial and cytotoxic activities, we report synthesis of novel Schiff base thiosemicarbazones and their metal (II) complexes of Co (II), Ni (II), Cu (II) and Zn (II) which exhibits high antitumor activities and low toxicity. For structural elucidations, various spectroscopic techniques (IR, UV–Vis, NMR, mass), elemental analyses, molar conductance, magnetic moment measurements and thermal methods were used. The biological activities were also screened against some bacterial and fungal organisms. Screening for antitumor activities was also done.

2 | EXPERIMENTAL

2.1 | Materials and methods

In the present work, all the chemicals used were of analytical reagent grade obtained from Sigma. They included 4-methyl-3-thiosemicarbazide, 2-hydroxy-1-naphthaldehyde, 4-hydroxy benzaldehyde, 3,5-dichlorosalicylaldehyde, propargyl bromide, bromomethyl benzene, (2-bromo-ethyl)-benzene, anhydrous potassium carbonate and transition metal (II) acetates Co $(CH_3COO)_2.4H_2O$, Ni $(CH_3COO)_2.4H_2O$, Cu $(CH_3COO)_2.H_2O$ and Zn $(CH_3COO)_2.2H_2O$. Organic solvents like methyl alcohol, hexane, chloroform and dimethylformamide were of spectroscopic purity and used as such without further purification. The starting materials 2-phenethyloxy-naphthalene-1-carbaldehyde (a), 2-benzyloxy-naphthalene-1-carbaldehyde (b), 4-prop-2-ynyloxy-benzaldehyde (c) and 2-benzyloxy-3,5-dichloro-benzaldehyde (d) were prepared by the methods reported in the literature.[30]

2.2 | Physicochemical measurements

The melting points (°C) were observed in open capillaries and are uncorrected. The Fourier transform infrared (FTIR) spectra were recorded on Shimadzu IR affinity-I 8000 FT-IR spectrometer using KBr pellets in the wavelength range of 4000–400 cm^{-1}. ^1H and ^{13}C NMR spectra were recorded on Bruker Avance II 400 MHz NMR spectrometer in $CDCl_3$ and DMSO-d_6 by using TMS as an internal standard (chemical shift (δ) in ppm, coupling constant J in (Hz)). Electronic spectra were recorded in DMF on UV–VIS–NIR Varian Cary-5000 spectrometer at room temperature. Magnetic susceptibilites of the complexes were measured at room temperature by using Gouy's method taking Hg [Co $(SCN)_4$] as the calibrant. Electron spin resonance spectra of the copper (II) complexes were recorded by using tetracyanoethylene (TCNE) as an internal standard on a Varian E112 X-band spectrometer. Molar conductance measurements of metal complexes in DMF (concentration 10^{-3} M) at room temperature were carried out using a model-306 Systronics conductivity bridge. Elemental analysis (C, H, N) was carried out on the instrument Perkin Elmer 2400. Thermogravimetric (TG) analysis of samples were carried out at a heating rate of 10 °C min^{-1} using Perkin Elmer Diamond TG/DTA thermogravimetric analyzer instrument at a flow rate of 20 mL min^{-1} under high purity argon atmosphere. Mass spectra were recorded on API 2000 (Applied Biosystems) mass spectrometer equipped with an electrospray source and a Shimadzu Prominence LC. Thin

layer chromatography (TLC) was run on the plates of readymade silica gel (SIL G/UV254, ALUGRAM) and visualized under ultraviolet light. The X-ray powder diffraction measurements were obtained using a Rigaku Table Top X-ray diffractometer at a scan rate of 2° min^{-1} in the range of $2\theta = 20–80°$.

2.3 | Synthesis of starting material - 2-Phenethyloxy-naphthalene-1-carbaldehyde (a), 2-Benzyloxy naphthalene-1-carbaldehyde (b), 4-Prop-2-ynyloxy-benzaldehyde (c) and 2-Benzyloxy-3,5-dichloro-benzaldehyde (d)

To the solution of 2-hydroxy-1-naphthaldehyde/3,5-dichlorosalicylaldehyde (1.0 mmol) in 20 ml DMF, anhydrous potassium carbonate (2.0 mmol) was added and stirred for 30 min. Then, slowly added (2-bromo-ethyl)-benzene (1.0 mmol) and bromomethyl-benzene (1.0 mmol) in DMF for product a, b and d. The reaction mixture and was further stirred for 24–48 hr. Feasibility of the reaction was frequently monitored by TLC. The solvent was evaporated and the resulting dark brown (a), light brown (b) and white colored (d) solid were washed with ice-cold water and recrystallized from chloroform.

To the solution of 4-hydroxy benzaldehyde (1.0 mmol) in 20 ml acetone, anhydrous potassium carbonate (2.0 mmol) was added and the resulting suspension was stirred and refluxed for 30 min. Then, (2.0 mmol) propargyl bromide (80% in toluene) was added to it slowly and the reaction mixture was further refluxed for 8 hr. The solvent was evaporated and resulting off white solid (c) was washed with ice-cold water and recrystallized by chloroform/hexane (scheme 1).

2.4 | Synthesis of Schiff base ligands L_1-L_4 (1–4)

4-methyl-3-thiosemicarbazide (3.0 mmol, 3.15 g) dissolved in about 20 ml hot methanol was added slowly to a magnetically stirred solution of above prepared derivatives of napthaldehyde/benzaldehyde (a,b,c,d) in equimolar ratio in the presence of few drops of glacial acetic acid and mixture was refluxed for 3–4 hr. Then, the solution was concentrated to its half volume and the obtained colored products were filtered off, washed several times with methanol and recrystallized from chloroform (scheme 2).

2.4.1 | (Z)-N-methyl-2-((2-phenethoxynaphthalen-1-yl)methylene) hydrazinecarbothioamide (L_1)

Dark brown; yield 80%; m.p. 125 °C; Anal. Calcd. for $C_{21}H_{21}N_3OS$: C, 69.41; H, 5.79; N, 11.57. Found: C, 69.39; H, 5.82; N, 11.56. Conductivity: (ohm^{-1} cm^2 mol^{-1}) in DMF: 12. IR (KBr, cm^{-1}): 1560 υ(C=N), 1270 υ(C=S), 3300 υ(N-H). ^1H NMR (400 MHz, $CDCl_3$) δ (ppm): 8.81 (s, 1H, -C=NH), 8.77 (d, 1H, -NH, $J = 8$ Hz), 8.06 (s, 1H, -NH), 7.89(d, 1H, Ar-H, J = 8 Hz), 7.82 (d, 1H, Ar-H, J = 8 Hz), 7.59–7.55(m, 1H, Ar-H), 7.46–7.26(m, 6H,

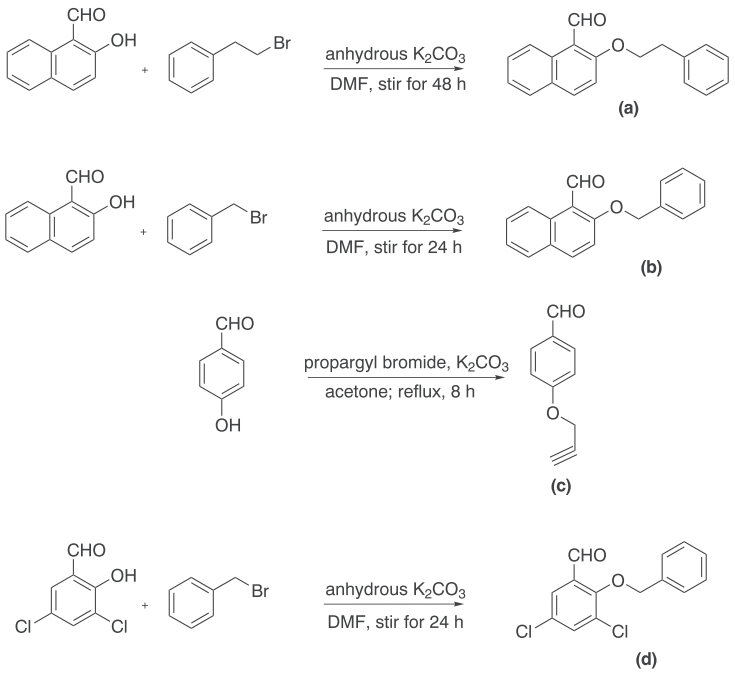

SCHEME 1 Synthesis of starting aldehydic derivatives

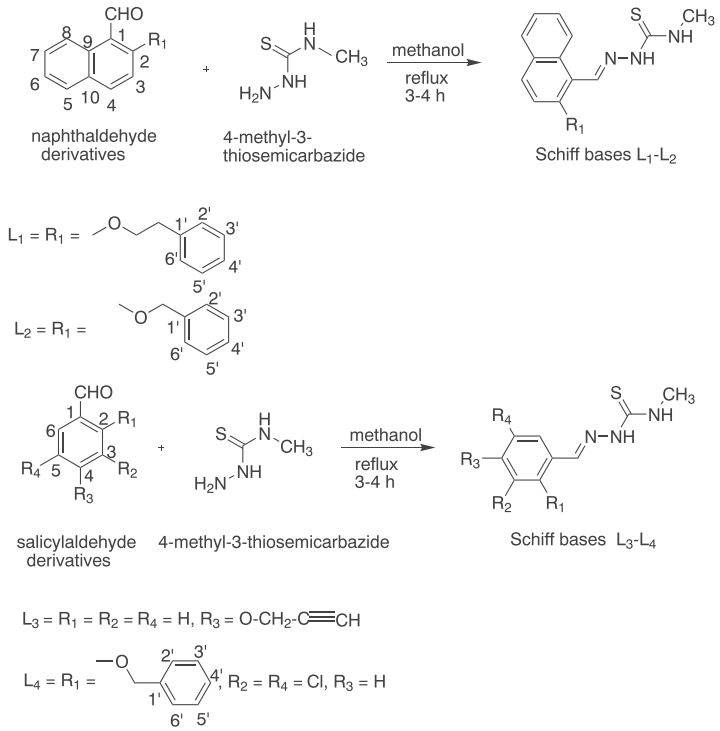

SCHEME 2 Scheme for synthesis of the Schiff base ligands L_1-L_4 (1–4)

Ar-H), 4.41(t, 2H, -OCH_2), 3.30(d, 3H, -CH_3), 3.19 (t, 2H, -CH_2), ^{13}C NMR (400 MHz, $CDCl_3$) δ (ppm): 178.49 (C=S), 157.43(C_2), 140.61 (-C=N-), 138.12(C_1), 132.69(C_9), 131.17(C_4), 129.45(C_{10}), 129.12(C_3,C_5), 128.81(C_5), 128.65(C_2,C_6), 128.13(C_7), 127.07(C_4), 124.94(C_6), 124.44(C_3), 115.38(C_8), 114.51(C_1), 70.81(-O-CH_2), 35.98 (-CH_2-Ar), 31.36 (-CH_3), ESI-MS (m/z): 364.11 $(M + H)^+$.

2.4.2 | (Z)-2-((2-(benzyloxy)naphthalen-1-yl)methylene)-N-methylhydrazinecarbothioamide (L_2)

Light brown; yield 84%; m.p. 130 °C; Anal. Calcd. for $C_{20}H_{19}N_3OS$: C, 68.72; H, 5.50; N, 2.04. Found: C, 68.74; H, 5.48; N, 2.02. Conductivity: (ohm^{-1} cm^2 mol^{-1}) in DMF: 13. IR (KBr, cm^{-1}): 1565 υ(C=N), 1273 υ(C=S), 3302 υ(N-H). ^{1}H NMR (400 MHz, $CDCl_3$) δ (ppm): 9.24(s, 1H, -C=NH-), 8.79(s, 1H, -NH), 8.57(s, 1H, -NH), 7.90(d, 1H, Ar-H, J = 8 Hz), 7.83(d, 1H, Ar-H, J = 8 Hz), 7.61–7.57(m, 1H, Ar-H), 7.46–7.39(m, 5H, Ar-H), 7.34(d, 1H, Ar-H, J = 8 Hz), 5.27(s, 2H, -OCH_2), 3.27(d, 3H, -CH_3), ^{13}C NMR (400 MHz, $CDCl_3$) δ (ppm): 178.43(-C=S), 157.16(C_2), 140.37(-C=N-), 136.21(C_1), 132.71(C_9), 131.36(C_4), 129.34(C_{10}), 128.86(C_3,C_5), 128.70(C_5), 128.43(C_2,C_6), 128.17(C_7), 127.57(C_4), 124.80(C_6), 124.40(C_3), 115.04(C_8), 114.10(C_1), 71.67(-O-CH_2), 31.36(-CH_3), ESI-MS (m/z): 350.22$(M + H)^+$.

2.4.3 | (E)-2-(4-(but-3-yn-1-yl) benzylidene)-N-methylhydrazinecarbothioamide (L_3)

White; yield 85%; m.p. 110 °C; Anal. Calcd. for $C_{12}H_{13}N_3OS$: C, 51.50; H, 5.38; N, 7.23. Found: C, 51.51; H, 5.36; N, 7.21. Conductivity: (ohm^{-1} cm^2 mol^{-1}) in DMF: 16. IR (KBr, cm^{-1}): 1565 υ(C=N), 1275 υ(C=S), 3309 υ(N-H). ^{1}H NMR (400 MHz, $CDCl_3$) δ (ppm): 9.38(s, 1H, -C=NH-), 7.78(s, 1H, -NH), 7.64(d, 2H, Ar-H, J = 8 Hz), 7.46(s, broad, 1H), 7.02(d, 2H, Ar-H, J = 8 Hz), 4.76(s, 2H, methylene), 3.28(d, 3H, CH_3 group), 2.57(s, 1H, −alkyne group), ^{13}C NMR (400 MHz, $CDCl_3$) δ (ppm): 178.25 (C=S), 159.22(C_4), 142.18 (-C=N-), 128.77(C_2, C_6), 127.01(C_1), 115.21(C_3, C_5), 78.01(-O-CH_2-alkyne), 75.98(alkyne), 55.86(methylene), 31.06(-CH_3), ESI-MS (m/z): 248.18 $(M + H)^+$.

2.4.4 | (Z)-2-(3,5-dichloro-2-phenethoxybenzylidene)-N-methylhydrazinecarbothioamide (L_4)

White; yield 87%; m.p. 165 °C; Anal. Calcd. for $C_{16}H_{15}Cl_2N_3OS$: C, 52.19; H, 4.12; N, 11.39. Found: C, 52.18; H, 4.11; N, 11.41. Conductivity: (ohm^{-1} cm^2 mol^{-1}) in DMF: 13. IR (KBr, cm^{-1}): 1568 υ(C=N), 1275 υ(C=S), 3308 υ(N-H). ^{1}H NMR (400 MHz, $CDCl_3$) δ (ppm): 9.11(s, 1H, -C=NH-), 7.69(s, 1H, Ar-H), 7.68(s, 1H,-NH, Ar-H), 7.49(s, 1H, Ar-H), 7.44–7.39(m, 4H, Ar-

H), 7.35(s, broad, -NH), 5.03(s, 2H, methylene, 3.25(d, 3H, $-CH_3$), ^{13}C NMR (400 MHz, $CDCl_3$) δ (ppm): 178.49 (-C=S), 152.34(C_2), 136.08(-C=N-), 135.34(C_1), 131.62(C_4), 130.22(C_3, C_5), 129.73(C_6), 129.04(C_2,C_6), 128.86(C_5), 128.83(C_4), 124.37(C_3), 117.57(C_1), 72.09($-OCH_2$), 31.93($-CH_3$), ESI-MS (m/z): 368.23$(M + H)^+$.

2.5 | Synthesis of transition metal (II) complexes (5–20)

The different complexes of transition metals were prepared by addition of metal acetates of Co (II), Ni (II), Cu (II) and Zn (II) (1.0 mmol) dissolved in about 20 ml methanol into 20 ml methanolic solution of above synthesized ligands (1.0 mmol) in 1:1 molar ratio. The mixture was stirred for 3–4 hr at room temperature by adjusting pH 4–5 by adding some drops of aqueous base *i.e.* NaOH. The different colored precipitates separated out were filtered, washed with hexane and finally recrystallized from chloroform and dried to get the pure product as represented in Scheme 3.

2.5.1 | $[co(L_1).(CH_3COO)_2.2H_2O]$ (5)

Brown Red; yield 72%; m.p. 265 °C; Anal. Calcd. for $C_{25}H_{31}N_3NiO_7S$: C, 52.14; H, 5.43; N, 7.31; Co, 10.20. Found: C, 52.10; H, 5.42; N, 7.29; Co, 10.18. Conductivity: (ohm^{-1} cm^2 mol^{-1}) in DMF: 18. IR (KBr, cm^{-1}): 3457 υ(H-O-H), 1549 υ(C=N), 1259 υ(C=S), 3278 υ(N-H), 1736 υ (CH_3COO), 435 υ(M-N), 403 υ(M-S). ESI-MS (m/z): 576.02$(M + H)^+$.

2.5.2 | $[Ni(L_1).(CH_3COO)_2.2H_2O]$ (6)

Green; yield 76%; m.p. 258 °C; Anal. Calcd. for $C_{36}H_{30}F_2N_2NiO_4$: C, 66.39; H, 4.64; N, 4.30; Ni, 9.01. Found: C, 66.43; H, 4.63; N, 4.27; Ni, 9.04. Conductivity: (ohm^{-1} cm^2 mol^{-1}) in DMF: 2.8. IR (KBr, cm^{-1}): 3460 υ(H-O-H), 1555 υ(C=N), 1254 υ(C=S), 3280 υ(N-H), 1740 υ (CH_3COO), 440 υ(M-N), 410 υ(M-S). ESI-MS (m/z): 651.86 $(M + H)^+$.

2.5.3 | $[cu(L_1).(CH_3COO)_2.2H_2O]$ (7)

Brown; yield 69%; m.p. 245 °C; Anal. Calcd. for $C_{25}H_{31}CuN_3O_7S$: C, 51.65; H, 5.40; N, 7.25; Cu, 10.95. Found: C, 51.67; H, 5.38; N, 7.23; Cu, 10.93. Conductivity: (ohm^{-1} cm^2 mol^{-1}) in DMF: 11. IR (KBr, cm^{-1}): 3410 υ(H-O-H), 1543 υ(C=N), 1250 υ(C=S), 3285 υ(N-H), 1744 υ (CH_3COO), 442 υ(M-N), 407 υ(M-S). ESI-MS (m/z): 583.03 $(M + H)^+$.

2.5.4 | $[Zn(L_1).(CH_3COO)_2.2H_2O]$ (8)

White; yield 71%; m.p. 265 °C; Anal. Calcd. for $C_{25}H_{31}N_3O_7SZn$: C, 51.49; H, 5.34; N, 7.23; Cu, 11.20. Found: C, 51.51; H, 5.36; N, 7.21; Cu, 11.22. Conductivity: (ohm^{-1} cm^2 mol^{-1}) in DMF: 2.8. IR (KBr, cm^{-1}): 3505 υ(H-O-H), 1550 υ(C=N), 1258 υ(C=S), 3283 υ(N-H), 1742 υ (CH_3COO), 439 υ(M-N), 400 υ(M-S). ^1H NMR (400 MHz, $CDCl_3$) δ (ppm): 8.78(s, 1H, -C=NH-), 8.74(d, 1H, -NH), 8.04(d, 1H, -NH-), 7.89 (d, 1H, Ar-H, J = 8 Hz), 7.82 (d, 1H, Ar-H, J = 8 Hz), 7.57(t, 1H, Ar-H, J = 8 Hz), 7.45–7.26(m, 6H, Ar-H), 4.41(t, 2H, $-OCH_2$), 3.30(d, 3H, $-CH_3$), 3.19(t, 2H, $-CH_2$), 2.38 (s, 6H, $-CH_3COO$). ^{13}C NMR (400 MHz, $CDCl_3$) δ (ppm):

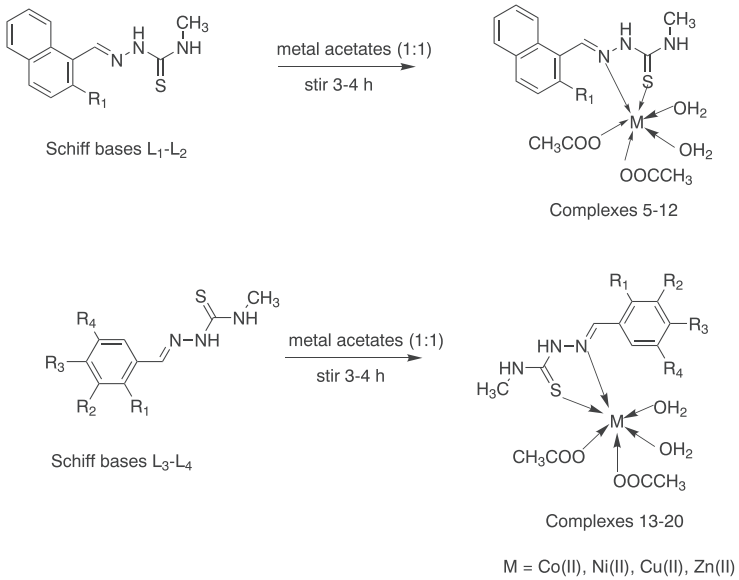

SCHEME 3 Scheme for the synthesis of Co (II), Ni (II), Cu (II) and Zn (II) complexes (5–20)

178.41 (C=S), 173.76(-COO), 157.43(C_2), 140.70 (-C=N-), 138.12(C_1), 132.69(C_9), 131.16(C_4), 129.43(C_{10}), 129.13(C_3,C_5), 128.81(C_5), 128.66(C_2,C_6), 128.13(C_7), 127.06(C_4), 124.95(C_6), 124.43(C_3), 115.34(C_8), 114.48(C_1), 70.80(-O-CH_2), 35.97(-CH_2-Ar), 31.38(-CH_3), 18.57(acetate methyl). ESI-MS (m/z): 265 $(M + H)^+$.

2.5.5 | $[co(L_2).(CH_3COO)_2.2H_2O]$ (9)

Brown Red; yield 72%; m.p. 275 °C; Anal. Calcd. for $C_{24}H_{29}CoN_3O_7S$: C, 51.23; H, 5.23; N, 7.43; Co, 10.45. Found: C, 51.25; H, 5.20; N, 7.47; Co, 10.48. Conductivity: (ohm^{-1} cm^2 mol^{-1}) in DMF: 16. IR (KBr, cm^{-1}): 3467 υ(H-O-H), 1542 υ(C=N), 1256 υ(C=S), 3288 υ(N-H), 1744 υ (CH_3COO), 436 υ(M-N), 408 υ(M-S). ESI-MS (m/z): 563.21$(M + H)^+$.

2.5.6 | $[Ni(L_2).(CH_3COO)_2.2H_2O]$ (10)

Green; yield 73%; m.p. 290 °C; Anal. Calcd. for $C_{24}H_{29}N_3NiO_7S$: C, 51.29; H, 5.16; N, 7.45; Ni, 10.41. Found: C, 51.27; H, 5.20; N, 7.47; Ni, 10.44. Conductivity: (ohm^{-1} cm^2 mol^{-1}) in DMF: 13. IR (KBr, cm^{-1}): 3498 υ(H-O-H), 1540 υ(C=N), 1249 υ(C=S), 3286 υ(N-H), 1740 υ (CH_3COO), 442 υ(M-N), 415 υ(M-S). ESI-MS (m/z): 562.21 $(M + H)^+$.

2.5.7 | $[cu(L_2).(CH_3COO)_2.2H_2O]$ (11)

Brown; yield 68%; m.p. 268 °C; Anal. Calcd. for $C_{24}H_{29}CuN_3O_7S$: C, 50.80; H, 5.12; N, 7.38; Cu, 11.23. Found: C, 50.83; H, 5.15; N, 7.41; Cu, 11.21. Conductivity: (ohm^{-1} cm^2 mol^{-1}) in DMF: 18. IR (KBr, cm^{-1}): 3512 υ(H-O-H), 1556 υ(C=N), 1247 υ(C=S), 3290 υ(N-H), 1737 υ (CH_3COO), 445 υ(M-N), 412 υ(M-S). ESI-MS (m/z): 567.10 $(M + H)^+$.

2.5.8 | $[Zn(L_2).(CH_3COO)_2.2H_2O]$ (12)

White; yield 73%; m.p. 270 °C; Anal. Calcd. for $C_{25}H_{31}N_3O_7SZn$: C, 50.63; H, 5.17; N, 7.34; Cu, 11.51. Found: C, 50.66; H, 5.14; N, 7.39; Cu, 11.49. Conductivity: (ohm^{-1} cm^2 mol^{-1}) in DMF: 11. IR (KBr, cm^{-1}): 3425 υ(H-O-H), 1554 υ(C=N), 1258 υ(C=S), 3284 υ(N-H), 1743 υ (CH_3COO), 441 υ(M-N), 404 υ(M-S). ^1H NMR (400 MHz, $CDCl_3$) δ (ppm): 9.22(s, 1H, -C=NH-), 8.77(s, 1H, -NH), 8.54(s, 1H, -NH), 7.87(d, 1H, Ar-H, J = 8 Hz), 7.80(d, 1H, Ar-H, J = 8 Hz), 7.57(t, 1H, Ar-H), 7.43–7.33 (m, 6H, Ar-H), 5.24(s, 2H, -OCH_2), 3.24(d, 3H, -CH_3), 2.38 (s, 6H, -CH_3COO). ^{13}C NMR (400 MHz, $CDCl_3$) δ (ppm): 178.37 (-C=S), 173.70(-COO), 157.10(C_2), 140.31 (-C=N-), 136.15(C_1), 132.65(C_9), 131.30(C_4), 129.28(C_{10}), 128.80(C_3,C_5), 128.64(C_5), 128.37(C_2,C_6), 128.12(C_7), 127.51(C_4), 124.74(C_6), 124.35(C_3), 114.98(C_8), 114.05(C_1), 71.62(-O-CH_2), 31.31(-CH_3), 18.49(acetate methyl). ESI-MS (m/z): 568.30$(M + H)^+$.

2.5.9 | $[co(L_3).(CH_3COO)_2.2H_2O]$ (13)

Brown Red; yield 77%; m.p. 280 °C; Anal. Calcd. for $C_{16}H_{23}CoN_3O_7S$: C, 41.76; H, 5.02; N, 9.10; Co, 12.83. Found: C, 41.74; H, 5.04; N, 9.13; Co, 12.80. Conductivity: (ohm^{-1} cm^2 mol^{-1}) in DMF: 12. IR (KBr, cm^{-1}): 3487 υ(H-O-H), 1544 υ(C=N), 1241 υ(C=S), 3288 υ(N-H), 1744 υ (CH_3COO), 450 υ(M-N), 412 υ(M-S). ESI-MS (m/z): 461.30 $(M + H)^+$.

2.5.10 | $[Ni(L_3).(CH_3COO)_2.2H_2O]$ (14)

Green; yield 72%; m.p. 290 °C; Anal. Calcd. for $C_{16}H_{23}N_3NiO_7S$: C, 41.77; H, 5.07; N, 9.12; Ni, 12.78. Found: C, 41.76; H, 5.04; N, 9.13; Ni, 12.76. Conductivity: (ohm^{-1} cm^2 mol^{-1}) in DMF: 17. IR (KBr, cm^{-1}): 3500 υ(H-O-H), 1533 υ(C=N), 1240 υ(C=S), 3279 υ(N-H), 1735 υ (CH_3COO), 446 υ(M-N), 408 υ(M-S). ESI-MS (m/z): 460.16 $(M + H)^+$.

2.5.11 | $[cu(L_3).(CH_3COO)_2.2H_2O]$ (15)

Brown; yield 68%; m.p. 270 °C; Anal. Calcd. for $C_{16}H_{23}CuN_3O_7S$: C, 41.32; H, 4.95; N, 9.06; Cu, 13.78. Found: C, 41.33; H, 4.99; N, 9.04; Cu, 13.67. Conductivity: (ohm^{-1} cm^2 mol^{-1}) in DMF: 13. IR (KBr, cm^{-1}): 3457 υ(H-O-H), 1548 υ(C=N), 1255 υ(C=S), 3280 υ(N-H), 1738 υ (CH_3COO), 438 υ(M-N), 405 υ(M-S). ESI-MS (m/z): 465.17 $(M + H)^+$.

2.5.12 | $[Zn(L_3).(CH_3COO)_2.2H_2O]$ (16)

White; yield 70%; m.p. 265 °C; Anal. Calcd. for $C_{16}H_{23}N_3O_7SZn$: C, 41.15; H, 4.98; N, 9.02; Cu, 14.03. Found: C, 41.17; H, 4.97; N, 9.00; Cu, 14.01. Conductivity: (ohm^{-1} cm^2 mol^{-1}) in DMF: 19. IR (KBr, cm^{-1}): 3515 υ(H-O-H), 1536 υ(C=N), 1260 υ(C=S), 3283 υ(N-H), 1742 υ (CH_3COO), 449 υ(M-N), 419 υ(M-S). ^1H NMR (400 MHz, $CDCl_3$) δ (ppm): 9.57(s, 1H, -C=NH-), 7.81(s, 1H, -NH), 7.62(d, 2H, Ar-H, J = 8 Hz), 7.47(s, broad, 1H), 7.02(d, 2H, Ar-H, J = 8 Hz), 4.76(s, 2H, methylene), 3.29(d, 3H, CH_3 group), 2.57(s, 1H, −alkyne group), 2.35 (s, 6H, -CH_3COO). ^{13}C NMR (400 MHz, $CDCl_3$) δ (ppm): 178.19 (C=S), 175.39(-COO), 159.34(C_4), 142.12 (-C=N-), 128.85(C_2, C_6), 126.78(C_1), 115.27(C_3, C_5),

77.98(-O-CH_2-alkyne), 76.02(alkyne), 55.87(methylene), 31.17(-CH_3), 19.62(acetate methyl). ESI-MS (m/z): 467.39$(M + H)^+$.

2.5.13 | [co(L_4).($CH_3COO)_2$.2H_2O] (17)

Brown Red; yield 77%; m.p. 275 °C; Anal. Calcd. for $C_{20}H_{25}Cl_2CoN_3O_7S$: C, 41.33; H, 4.36; N, 7.25; Co, 10.13. Found: C, 41.32; H, 4.33; N, 7.23; Co, 10.14. Conductivity: (ohm^{-1} cm^2 mol^{-1}) in DMF: 20. IR (KBr, cm^{-1}): 3424 υ(H-O-H), 1549 υ(C=N), 1250 υ(C=S), 3287 υ(N-H), 1744 υ (CH_3COO), 442 υ(M-N), 410 υ(M-S). ESI-MS (m/z): 581.06 $(M + H)^+$.

2.5.14 | [Ni(L_4).($CH_3COO)_2$.2H_2O] (18)

Light Brown; yield 70%; m.p. 285 °C; Anal. Calcd. for $C_{20}H_{25}Cl_2N_3NiO_7S$: C, 41.37; H, 4,35; N, 7.24; Ni, 10.09. Found: C, 41.34; H, 4.34; N, 7.23; Ni, 1o.10. Conductivity: (ohm^{-1} cm^2 mol^{-1}) in DMF: 14. IR (KBr, cm^{-1}): 3490 υ(H-O-H), 1542 υ(C=N), 1240 υ(C=S), 3290 (N-H), 1739 υ (CH_3COO), 436 υ(M-N), 420 υ(M-S). ESI-MS (m/z): 580.33 $(M + H)^+$.

2.5.15 | [cu(L_4).($CH_3COO)_2$.2H_2O] (19)

Green; yield 718%; m.p. 270 °C; Anal. Calcd. for $C_{20}H_{25}Cl_2CuN_3O_7S$: C, 41.02; H, 4.27; N, 7.13; Cu, 10.86. Found: C, 41.00; H, 4.30; N, 7.17; Cu, 10.85. Conductivity: (ohm^{-1} cm^2 mol^{-1}) in DMF: 11. IR (KBr, cm^{-1}): 3478 υ(H-O-H), 1534 υ(C=N), 1248 υ(C=S), 3281 υ(N-H), 1743 υ (CH_3COO), 440 υ(M-N), 408 υ(M-S). ESI-MS (m/z): 585.52 $(M + H)^+$.

2.5.16 | [Zn(L_4).($CH_3COO)_2$.2H_2O] (20)

White; yield 69%; m.p. 265 °C; Anal. Calcd. for $C_{20}H_{25}Cl_2N_3O_7SZn$: C, 40.88; H, 4.30; N, 7.18; Cu, 11.11. Found: C, 40.87; H, 4.29; N, 7.15; Cu, 11.12. Conductivity: (ohm^{-1} cm^2 mol^{-1}) in DMF: 16. IR (KBr, cm^{-1}): 3446 υ(H-O-H), 1537 υ(C=N), 1251 υ(C=S), 3290 υ(N-H), 1744 υ (CH_3COO), 445 υ(M-N), 416 υ(M-S). ^{1}H NMR (400 MHz, $CDCl_3$) δ (ppm): 8.84(s, 1H, -C=NH-), 7.67(s, 1H, Ar-H), 7.65(s, 1H,N-NH-), 7.47(d, 1H, Ar-H, J = 8 Hz), 7.42–7.38(m, 3H, Ar-H), 7.36(s, 1H,N-NH-), 5.01(s, 2H, methylene), 3.24(d, 3H, -CH_3), 2.40 (s, 6H, CH_3COO). ^{13}C NMR (400 MHz, $CDCl_3$) δ (ppm): 178.58 (-C=S), 173.89(-COO), 152.34 (C_2), 136.06(-C=N-), 135.34(C_1), 131.62(C_4), 130.23(C_3, C_5), 130.21(C_6), 129.72(C_2,C_6), 129.05(C_5), 128.84(C_4), 124.37(C_3), 117.21(C_1), 72.39(-OCH_2), 31.96(-CH_3), 19.23(acetate methyl). ESI-MS (m/z): 586.11$(M + H)^+$.

2.6 | Biophysical experiments

2.6.1 | Methodology of antimicrobial activities

In vitro antimicrobial activity of the compounds were tested by the standard serial dilution method against four bacterial strains *i.e*. Gram-positive bacteria *Staphylococcus aureus* (MTCC 2901), *Streptococcus gordonii* (MTCC 822); Gram-negative bacteria *Escherichia coli* (MTCC 16521), *Pseudomonas aeruginosa* (MTCC 424); two fungus strains *Candida albicans* (MTCC 227) and *Aspergillus niger* (MTCC 8189) which were cultured on nutrient broth and potato dextrose broth as nutrient medium. Ciprofloxacin and fluconazole were used as standards for antimicrobial studies and the minimum inhibitory concentrations (MIC) were reported in μM/ml. MIC is the lowest concentration of any antimicrobial agent that will inhibits the visible growth of microorganisms after incubation at the optimum conditions and calculated by means of two fold serial dilution method using stock solution of test compounds having concentration 100 μg/ml in DMSO.[31] The stock solution was further diluted to make concentrations of 50, 25, 12.5, 6.25, 3.12, 1.56 and 0.75 μg/ml. The revived bacterial and fungal strains were inoculated to each serially diluted solution and kept in incubator at 37 °C for 24 hr in the case of the bacteria and at 25 °C for 7 days in case of the fungi. Then, the results were compared with that of standard reference drug.

2.6.2 | Cytotoxic assay

All the synthesized complexes and ligands were assessed for cytotoxicity against four different human cell lines: A549 derived from human alveolar adenocarcinoma epithelial cells (ATCC No. CCL-185); MCF7 derived from human breast adenocarcinoma cell line (ATCC No. MDA-MB-231); DU145 derived from human prostate cancer cells (ATCC No. HTB-81) and MRC-5 derived from human normal lung cells (ATCC No. CCL-171) by means of MTT colorimetric assay and using doxorubicin (Adriamycin) as a standard.[32] The growth inhibition of tumor cell lines was precise in different 96 well diffused plates by cell mediated reduction of tetrazolium salt to water insoluble formazan crystals. The consequence of different synthesized Schiff bases and metal complexes on the probability of cancer cell lines along with normal cell line was calculated on a multimode reader (InfiniteM200, Tecan, Mannedorf, Switzerland) at 540 nm wavelength.

The values obtained were corrected by subtracting the absorbance of background from that of the blanks. The dose response curves were plotted for the test compounds along with controls and their IC_{50} values in μM were calculated, which concerns with the concentration required to cause toxic effects in 50% of cells. The entire experiment was performed in triplicate.[33]

3 | RESULTS AND DISCUSSION

The Schiff base ligands (L_1-L_4) were obtained in good yield through the reaction of synthesized napthaldehyde/benzaldehyde/salicylaldehyde derivatives with 4-methyl-3-thiosemicarbazide in dry methanol with 1–2 drops of glacial acetic acid. The homogeneity of these compounds was regularly checked by TLC. Transition metal complexes formulated as $[M(L_{1-4}).(CH_3COO)_2.2H_2O]$ were synthesized by refluxing metal (II) acetates with Schiff bases using methanol in 1:1 molar ratio. The mode of bonding, denticity and the geometry of the complexes were elucidated by various spectroscopic techniques like NMR, FT-IR, mass, electronic spectra, ESR etc. The analytical data suggested the formation of different colored solid complexes, stable at room temperature and non-electrolytic in nature as the molar conductance values of the complexes were found to be in between 11–20 $ohm^{-1}cm^2mol^{-1}$.[34,35] All the compounds were soluble in MeOH, EtOH, $CDCl_3$, DMF and DMSO but were insoluble in water. The ligands were chelated to all metal ions via nitrogen atom of azomethine group and sulphur atom of thionyl group in thione form without the replacement of hydrogen atom. The physical measurements and analytical data of compounds **1–20** are depicted in Table 1.

3.1 | FT-IR spectra

In order to know the nature of functional groups and to interpret the coordinating mode of Schiff base ligands with metal ions in complexes, IR spectrum of Schiff bases and their complexes were recorded and compared with each other and the values are listed in Table 2. The IR spectrum of Schiff bases show bands in the region of 3300–3308 cm^{-1} assigned for υ (NH-) stretching vibrations, which shows downward shifting near 3278–3290 cm^{-1} indicating binding of Schiff bases through sulphur atom

TABLE 1 Analytical and physical data of the synthesized compounds

Sr. No.	Molecular formula	Yield (%)	Color	Found C	Found H	(Calcd.) N	% M	m/z	$(\Omega_M) \times 10^{-3}$ $\Omega^{-1}mol^{-1}cm^2$	M.P. (°C)
1	$C_{21}H_{21}N_3OS$	80	Dark brown	69.39 (69.41)	5.82 (5.79)	11.56 (11.57)	-	364.11	12	125
2	$C_{20}H_{19}N_3OS$	84	Light brown	68.74 (68.72)	5.48 (5.50)	12.02 (12.04)	-	350.22	13	130
3	$C_{12}H_{13}N_3OS$	85	White	51.51 (51.50)	5.36 (5.38)	7.21 (7.23)	-	248.18	16	110
4	$C_{16}H_{15}Cl_2N_3OS$	87	White	52.18 (52.19)	4.11 (4.12)	11.41 (11.39)	-	368.23	13	165
5	$C_{25}H_{31}CoN_3O_7S$	72	Brown red	52.08 (52.09)	5.42 (5.41)	7.29 (7.28)	10.22 (10.19)	577.85	15	265
6	$C_{25}H_{31}N_3NiO_7S$	76	Green	52.10 (52.14)	5.42 (5.43)	7.29 (7.31)	10.18 (10.20)	576.02	18	258
7	$C_{25}H_{31}CuN_3O_7S$	69	Brown	51.67 (51.65)	5.38 (5.40)	7.23 (7.25)	10.93 (10.95)	583.03	11	245
8	$C_{25}H_{31}N_3O_7SZn$	71	White	51.51 (51.49)	5.36 (5.34)	7.21 (7.23)	11.22 (11.20)	582.22	12	265
9	$C_{24}H_{29}CoN_3O_7S$	72	Brown red	51.25 (51.23)	5.20 (5.23)	7.47 (7.43)	10.48 (10.45)	563.21	16	275
10	$C_{24}H_{29}N_3NiO_7S$	73	Green	51.27 (51.29)	5.20 (5.16)	7.47 (7.45)	10.44 (10.41)	562.21	13	290
11	$C_{24}H_{29}CuN_3O_7S$	68	Brown	50.83 (50.80)	5.15 (5.12)	7.41 (7.38)	11.21 (11.23)	567.10	18	268
12	$C_{24}H_{29}N_3O_7SZn$	73	White	50.66 (50.63)	5.14 (5.17)	7.39 (7.34)	11.49 (11.51)	568.30	11	270
13	$C_{16}H_{23}CoN_3O_7S$	77	Brown red	41.74 (41.76)	5.04 (5.02)	9.13 (9.10)	12.80 (12.83)	461.30	12	280
14	$C_{16}H_{23}N_3NiO_7S$	72	Green	41.76 (41.77)	5.04 (5.07)	9.13 (9.12)	12.76 (12.78)	460.16	17	290
15	$C_{16}H_{23}CuN_3O_7S$	68	Brown	41.33 (41.32)	4.99 (4.95)	9.04 (9.06)	13.67 (13.78)	465.17	`13	270
16	$C_{16}H_{23}N_3O_7SZn$	70	White	41.17 (41.15)	4.97 (4.98)	9.00 (9.02)	14.01 (14.03)	467.39	19	265
17	$C_{20}H_{25}Cl_2CoN_3O_7S$	77	Brown red	41.32 (41.33)	4.33 (4.36)	7.23 (7.25)	10.14 (10.13)	581.06	20	275
18	$C_{20}H_{25}Cl_2N_3NiO_7S$	70	Light brown	41.34 (41.37)	4.34 (4.35)	7.23 (7.24)	10.10 (10.09)	580.33	14	285
19	$C_{20}H_{25}Cl_2CuN_3O_7S$	71	Green	41.00 (41.02)	4.30 (4.27)	7.17 (7.13)	10.85 (10.86)	585.52	11	270
20	$C_{20}H_{25}Cl_2N_3O_7SZn$	69	White	40.87 (40.88)	4.29 (4.30)	7.15 (7.18)	11.12 (11.11)	586.11	16	265

in thione form without formation of thio-enol tautomer or no disappearance of υ(N-H) band. The bands in the region 1560–1568 cm^{-1} and 1270–1275 cm^{-1}, were observed in Schiff base spectra assigned for azomethine υ(-C=NH) and thiocarbonyl υ(C=S) stretching vibrations,[36] underwent modest downward shifting (bathochromic shift) by 20–25 cm^{-1} while comparing with the spectra of complexes and observed in the range of 1535–1556 and 1260–1240 cm^{-1}.[37] This shifting divulges donation of the lone pair of electrons available on azomethine nitrogen to metal centers and confirms binding through nitrogen and sulphur donor atoms.[38–40] In addition, new broad bands displayed near 3515–3410 cm^{-1} in all complexes may be attributed for two coordinated water molecules.

The bands observed near 435–450 cm^{-1} and 400–420 cm^{-1} which were not present in the free Schiff base ligands were assigned for formation of new bonds in the spectra of complexes ascribed as υ(M–N) and υ(M–S), reveals bidentate nature of Schiff bases and confirms coordination *via* S and N donor atoms.[41–43] Furthermore, another sharp peak was observed in the region ~1735–1744 cm^{-1} in all the 1:1 metal complexes, attributed due to υ ($OCOCH_3$) group which shows binding of acetate groups to the metal centers to complete their octahedral geometry.[44] In conclusion, the IR data suggests a bidentate nature of ligands.

3.2 | ^{1}H NMR spectra

The ^{1}H NMR spectrum of the Schiff bases and their respective transition metal (II) complexes were carried out in $CDCl_3$. The observed values of NMR data are given in experimental section and Figure 1. Schiff bases (L_1-L_4) showed a characteristic signal due to azomethine nitrogen in the range of δ 9.38–8.81 ppm. Another signal due to –NH proton adjacent to thionyl group appears near δ 8.79–7.68 ppm. Further, a broad signal in Schiff bases is observed towards the upfield region in the range of δ 8.57–7.35 ppm attributed to another –NH group which is attached to methyl group.[45] One sharp characteristic singlet near δ 5.27–4.41 ppm assigned for the protons of methylene group attached to oxygen atom (O-CH_2). A doublet in the range of δ 3.30–3.25 ppm was ascribed to the protons of methyl (-CH_3) group was observed in all ligands[46] and another triplet was observed in the case of ligand (L_1) at δ 3.19 ppm certified the presence of another methylene group. While in Schiff base L_3, a sharp singlet at δ 2.57 ppm was observed, revealed the presence

TABLE 2 Characteristic IR frequencies (cm^{-1}) of Schiff bases and their respective transition metal (II) complexes

S. No	Compounds	υ(H-O–H) water	υ(N–H)	υ(C=S)	υ (CH_3COO)	υ(-C=NH-) azomethine	υ(M-N)	υ(M–S)
1	L_1	-	3300	1270	-	1560	-	-
2	L_2	-	3302	1273	-	1564	-	-
3	L_3	-	3309	1275	-	1565	-	-
4	L_4	-	3308	1275	-	1568	-	-
5	$Co(L_1).(CH_3COO)_2.2H_2O$	3457	3278	1259	1736	1549	435	403
6	$Ni(L_1).(CH_3COO)_2.2H_2O$	3460	3280	1254	1740	1555	440	410
7	$Cu(L_1).(CH_3COO)_2.2H_2O$	3410	3285	1250	1744	1543	442	407
8	$Zn(L_1).(CH_3COO)_2.2H_2O$	3505	3283	1258	1742	1550	439	400
9	$Co(L_2).(CH_3COO)_2.2H_2O$	3467	3288	1256	1744	1542	436	408
10	$Ni(L_2).(CH_3COO)_2.2H_2O$	3498	3286	1249	1740	1540	442	415
11	$Cu(L_2).(CH_3COO)_2.2H_2O$	3512	3290	1247	1737	1556	445	412
12	$Zn(L_2).(CH_3COO)_2.2H_2O$	3425	3284	1258	1743	1554	441	404
13	$Co(L_3).(CH_3COO)_2.2H_2O$	3487	3288	1241	1744	1544	450	412
14	$Ni(L_3).(CH_3COO)_2.2H_2O$	3500	3279	1240	1735	1533	446	408
15	$Cu(L_3).(CH_3COO)_2.2H_2O$	3457	3280	1255	1738	1548	438	405
16	$Zn(L_3).(CH_3COO)_2.2H_2O$	3515	3283	1260	1742	1536	449	419
17	$Co(L_4).(CH_3COO)_2.2H_2O$	3424	3287	1250	1744	1549	442	410
18	$Ni(L_4).(CH_3COO)_2.2H_2O$	3490	3290	1240	1739	1542	436	420
19	$Cu(L_4).(CH_3COO)_2.2H_2O$	3478	3281	1248	1743	1534	440	408
20	$Zn(L_4).(CH_3COO)_2.2H_2O$	3446	3290	1251	1744	1537	445	416

TABLE 3 Electronic spectral data and magnetic moment (BM) of Schiff bases and their respective transition metal (II) complexes

Compounds	Absorption (cm^{-1})	Band assignment	Dq (cm^{-1})	B (cm^{-1})	β	β %	υ_2/υ_1	Geometry	μ (BM)
L_1	28,770 39,300	n → π π → π*	-	-	-	-	-	-	-
L_2	27,980 38,850	n → π π → π*	-	-	-	-	-	-	-
L_3	27,820 39,950	n → π π → π*	-	-	-	-	-	-	-
L_4	28,980 40,000	n → π π → π*	-	-	-	-	-	-	-
$Co(L_1).(CH_3COO)_2.2H_2O$	9,740 17,610 22,580	$^4T_{1g}(F) \rightarrow {}^4T_{2g}(F)$ (υ_1) $^4T_{1g}(F) \rightarrow {}^4A_{2g}(F)$ (υ_2) $^4T_{1g}(F) \rightarrow {}^4T_{2g}(P)$ (υ_3)	1284	707.3	0.728	27.2	2.31	Octahedral	4.45
$Ni(L_1).(CH_3COO)_2.2H_2O$	10,396 18,300 24,325	$^3A_{2g}(F) \rightarrow {}^3T_{2g}(F)$ (υ_1) $^3A_{2g}(F) \rightarrow {}^3T_{1g}(F)$ (υ_2) $^3A_{2g}(F) \rightarrow {}^3T_{1g}(P)$ (υ_3)	1039	762.4	0.732	26.8	1.76	Octahedral	3.23
$Cu(L_1).(CH_3COO)_2.2H_2O$	15,475 24,450	$^2B_1g \rightarrow {}^2A_1g$ (ν_1) $^2B_1g \rightarrow {}^2E_2g$ (ν_2)	-	-	-	-	-	Octahedral	1.92
$Zn(L_1).(CH_3COO)_2.2H_2O$	23,600	LMCT	-	-	-	-	-	Octahedral	-
$Co(L_2).(CH_3COO)_2.2H_2O$	9,810 17,585 22,494	$^4T_{1g}(F) \rightarrow {}^4T_{2g}(F)$ (υ_1) $^4T_{1g}(F) \rightarrow {}^4A_{2g}(F)$ (υ_2) $^4T_{1g}(F) \rightarrow {}^4T_{2g}(P)$ (υ_3)	1268.4	709.6	0.731	26.9	2.29	Octahedral	4.43
$Ni(L_2).(CH_3COO)_2.2H_2O$	10,285 18,460 24,220	$^3A_{2g}(F) \rightarrow {}^3T_{2g}(F)$ (υ_1) $^3A_{2g}(F) \rightarrow {}^3T_{1g}(F)$ (υ_2) $^3A_{2g}(F) \rightarrow {}^3T_{1g}(P)$ (υ_3)	1028	788.3	0.757	24.3	1.79	Octahedral	3.29
$Cu(L_2).(CH_3COO)_2.2H_2O$	15,330 24,850	$^2B_1g \rightarrow {}^2A_1g$ (ν_1) $^2B_1g \rightarrow {}^2E_2g$ (ν_2)	-	-	-	-	-	Octahedral	1.82
$Zn(L_2).(CH_3COO)_2.2H_2O$	23,890	LMCT	-	-	-	-	-	Octahedral	-
$Co(L_3).(CH_3COO)_2.2H_2O$	9,989 17,635 22,275	$^4T_{1g}(F) \rightarrow {}^4T_{2g}(F)$ (υ_1) $^4T_{1g}(F) \rightarrow {}^4A_{2g}(F)$ (υ_2) $^4T_{1g}(F) \rightarrow {}^4T_{2g}(P)$ (υ_3)	1228.6	669.5	0.689	31.1	2.22	Octahedral	4.48
$Ni(L_3).(CH_3COO)_2.2H_2O$	10,415 18,590 24,485	$^3A_{2g}(F) \rightarrow {}^3T_{2g}(F)$ (υ_1) $^3A_{2g}(F) \rightarrow {}^3T_{1g}(F)$ (υ_2) $^3A_{2g}(F) \rightarrow {}^3T_{1g}(P)$ (υ_3)	1041	788.6	0.758	24.2	1.78	Octahedral	3.22
$Cu(L_3).(CH_3COO)_2.2H_2O$	15,530 24,500	$^2B_1g \rightarrow {}^2A_1g$ (ν_1) $^2B_1g \rightarrow {}^2E_2g$ (ν_2)	-	-	-	-	-	Octahedral	1.89
$Zn(L_3).(CH_3COO)_2.2H_2O$	23,480	LMCT	-	-	-	-	-	Octahedral	-
$Co(L_4).(CH_3COO)_2.2H_2O$	9,625 17,350 22,390	$^4T_{1g}(F) \rightarrow {}^4T_{2g}(F)$ (υ_1) $^4T_{1g}(F) \rightarrow {}^4A_{2g}(F)$ (υ_2) $^4T_{1g}(F) \rightarrow {}^4T_{2g}(P)$ (υ_3)	1276.5	722.0	0.743	25.7	2.32	Octahedral	4.46
$Ni(L_4).(CH_3COO)_2.2H_2O$	10,510 18,420 24,390	$^3A_{2g}(F) \rightarrow {}^3T_{2g}(F)$ (υ_1) $^3A_{2g}(F) \rightarrow {}^3T_{1g}(F)$ (υ_2) $^3A_{2g}(F) \rightarrow {}^3T_{1g}(P)$ (υ_3)	1051	752.4	0.723	27.7	1.75	Octahedral	3.25
$Cu(L_4).(CH_3COO)_2.2H_2O$	15,275 24,300	$^2B_1g \rightarrow {}^2A_1g$ (ν_1) $^2B_1g \rightarrow {}^2E_2g$ (ν_2)	-	-	-	-	-	Octahedral	1.84
$Zn(L_4).(CH_3COO)_2.2H_2O$	23,780	LMCT	-	-	-	-	-	Octahedral	-

of alkyne proton. Further, some singlets, doublets and multiplets for aromatic protons were observed near δ 7.90–7.02 ppm.

On comparing the proton NMR of Schiff bases with their Zn (II) complexes, it was found that no change in the number of signals was observed, which confirms that

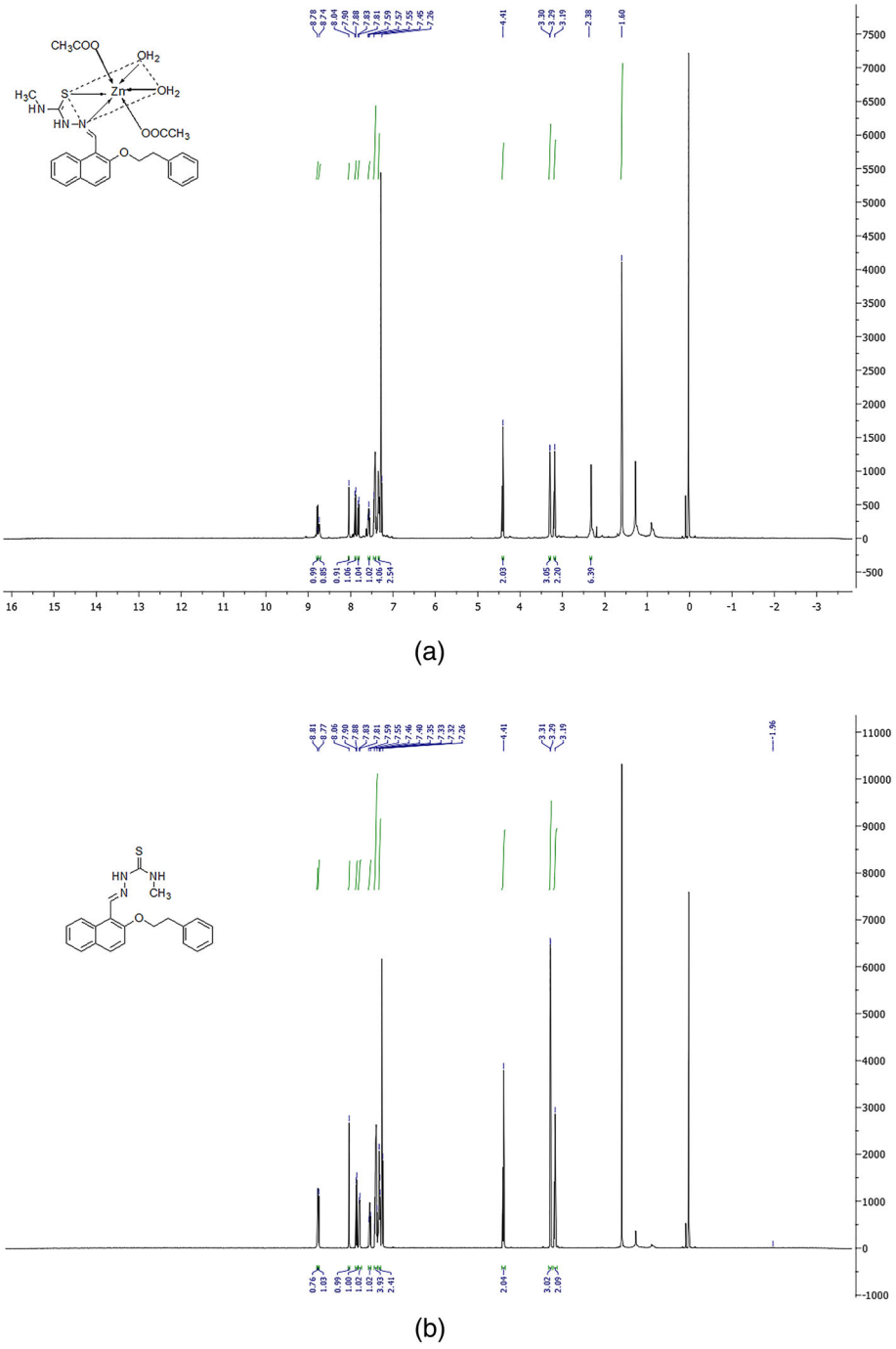

FIGURE 1 1H NMR spectra of (a) Schiff base 1 and (b) its zinc (II) complex (8)

the coordination of ligands to the metal ions has occurred through sulfur atom in thione form which reveals that there is no deprotonation of hydrazide nitrogen atom for thiolization of C=S group on complexation.[47] Further, shifting in the peaks of azomethine group appears in vicinity of δ 9.57–8.78 ppm indicates binding of ligands through azomethine nitrogen atom to the central metal ions. Moreover, the shifting without disappearance of signal assigned for –NH protons attached to thione group confirms the chelation via sulphur atom as it is in thione form.[48] Another signal due to –NH group attached to methyl groups also gets slightly shifted in spectra of complexes. Signals due to methyl, methylene, alkyne and aromatic protons were also slightly altered, resulting in complexation of Schiff bases to the metal ions.

3.3 | ^{13}C NMR spectra

^{13}C NMR spectra of Schiff bases and Zn (II) metal complexes were recorded in $CDCl_3$ and DMSO-d_6 using tetramethylsilane (TMS) as an internal standard and the

values are listed in experimental section and Figure 2. ^{13}C NMR spectrum of Schiff bases displayed characteristic signal in the range δ 152.34–159.22 ppm attributed to azomethine carbon (-C=N-) which underwent shifting in the complexes revealed binding of azomethine nitrogen atom via lone pair of electrons to the central metal ion.[49] A singlet near δ 178.49–178.25 ppm corresponding to the thionyl (-C=S) group gets shifted in the complexes confirming ligation through sulfur atom of Schiff bases to metal ions. The peaks due to aromatic carbons were observed near δ 142.18–114.10 ppm, exhibits alternation in the complexes as a result of coordination with metals.[50] A singlet in the vicinity of δ 31.93–31.06 ppm was observed due to methyl carbons adjacent to –NH group. The peaks for methylene carbons attached to oxygen atom appeared near δ 55.86–72.09 ppm. In L_1 ligand, an extra peak at δ 35.98 assigned for another methylene group present in the moiety, while in L_3, two more peaks were observed which were ascribed for alkyne carbons had been shifted to δ 77.98 and 76.02 ppm in the complexes. All values related to synthesized Schiff bases and their zinc (II) complexes are depicted in supplementary data.

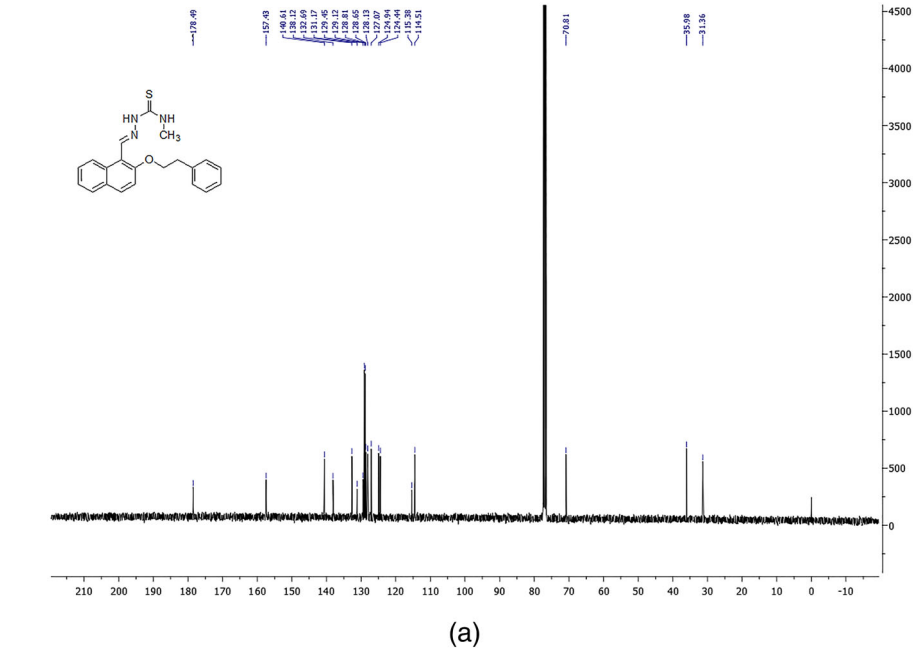

FIGURE 2 13C NMR spectra of (a) Schiff base (1) and (b) its zinc (II) complex (8)

3.4 | Mass spectra

The mass spectral data of Schiff base ligands and their metal chelates were specified in Table 1 and the peaks are shown in Figure 3. The molecular ion peaks are found in good agreement with the expected values. The mass spectrum of ligand L_1 gives a peak at 364.41 m/z, which is assigned for [M + H] peak and is in good agreement with the molecular weight of the compound 363.14. Co (II) complex of Schiff base L_1 gives molecular ion peak at m/z 577.85 assigned for [M + H] peak and was in good agreement with that of its molecular mass 576.12. Thus, the mass spectral results along with elemental analyses agreed with the formation of the complexes of type $[M(L)(CH_3COO)_2.2H_2O]$ in 1:1 stoichiometry.[39]

3.5 | Electronic spectra and magnetic measurements

The electronic spectra and magnetic moment measurements were recorded in solid state at room temperature in DMF in order to acquire the geometry of the complexes and the values obtained were summarized in Table 3. The electronic spectra of all Schiff bases showed two bands, one within the range of 27,820–28,980 cm^{-1} attributed to the n–π* transitions and another band within the range of 38,850–40,000 cm^{-1} is due to the π–π* transitions.[51]

The electronic spectra of the Co (II) complexes showed three bands around 9,625–9,989 cm^{-1}, 17,350–17,635 cm^{-1} and 22,275–22,580 cm^{-1} have been assigned for the $^4T_1g(F) \rightarrow {}^4T_2g(F)$, $^4T_1g(F) \rightarrow {}^4A_2g(F)$, $^4T_1g(F) \rightarrow {}^4T_1g(P)$ transitions, respectively which are characteristic of octahedral geometry.[52] The octahedral geometry for Co (II) complexes was further supported by the values obtained by the ratio of υ_2/υ_1, which lies within the range of 2.22–2.32 and various ligand field parameters like Dq, B, β and β% calculated by using band fitting equation. The values of B and nephelauxetic parameter β were found to be 669–722 cm^{-1} and 0.689–0.743, respectively. The B values were less than the free ion value (971 cm^{-1}) calculated from B (complex)/B (free ion), indicated covalent character between metal–ligand bonds. At room temperature, the magnetic moment values of the Co (II) complexes lie in the range of 4.43–4.48 BM due to three unpaired electrons and were in good agreement with those reported for the octahedral structure.[53]

Ni (II) complexes exhibited three bands in the vicinity of 10,285–10,510 cm^{-1}, 18,300–18,590 cm^{-1} and 24,220–24,485 cm^{-1} attributed to the $^3A_2g(F) \rightarrow {}^3T_2g(F)$, $^3A_1g(F) \rightarrow {}^3T_1g(F)$, $^3A_2g(F) \rightarrow {}^3T_1g(P)$ transitions respectively, and the value of υ_2/υ_1 was found to be 1.75–1.79, which were in harmony with octahedral geometry around nickel (II) ions. The Racah interelectronic repulsion parameters B, β were calculated for Ni (II) complexes and were found to be in the range 752–788 cm^{-1} and 0.723–0.758, respectively. The value of B was found to be less than the free ion value (1041 cm^{-1}) because of decreased interelectronic repulsions due to electron delocalization and shows covalent nature of bond between metal and ligand.[54] Further, the magnetic moment values for Ni (II) complexes were found near 3.22–3.29 BM, expected for S = 1 due to two unpaired electrons with small contribution of orbital motion also confirms octahedral geometry.[55]

In the electronic spectra of Cu (II) complexes, UV spectral bands were observed in vicinity of 15,275–15530 cm^{-1} and 24,300–24,850 cm^{-1} which were attributed for $^2B_1g \rightarrow {}^2A_1g\ (\nu_1)$ $^2B_1g \rightarrow {}^2E_2g\ (\nu_2)$ transitions, respectively and the magnetic moment values lies in the range of 1.82–1.92 BM corresponds to octahedral geometry.[56,57]

Zn (II) complexes exhibited only one band in the region of 23,480–23,890 cm^{-1} due to ligand to metal charge transfer transitions. Further, Zn (II) complexes are diamagnetic with fully filled d^{10} configuration and do not show any d-d transitions. On the basis of the above observations and spectral data, it was suggested that all the metal complexes possess octahedral geometry.[58] The figure representing electronic spectra of Schiff base L_2 and its metal (II) complexes is provided in supplementary data.

TABLE 4 ESR spectral parameters of Cu (II) complexes

Cu (II) complexes	$g_{\|\|}$	$g_\perp$	g_{av}	G
$Cu(L_1).(CH_3COO)_2.\ 2H_2O$	2.20	2.07	2.11	2.92
$Cu(L_2).(CH_3COO)_2.\ 2H_2O$	2.23	2.07	2.12	3.36
$Cu(L_3).(CH_3COO)_2.\ 2H_2O$	2.21	2.06	2.11	3.59
$Cu(L_4).(CH_3COO)_2.\ 2H_2O$	2.22	2.08	2.12	2.80

3.6 | ESR spectra

Electron spin resonance (ESR) is a branch of spectroscopy in which radiations in the range of microwave frequency was absorbed by molecules possessing electrons with unpaired spins. The solid state ESR spectrum of the Cu (II) complex was recorded at room temperature from which, $g_{||}$and g⊥values of $[Cu(L_2).(CH_3COO)_2.2H_2O]$ were calculated and shown in Figure 4. The spin Hamiltonian parameters of Cu (II) complexes were calculated and summarized in the Table 4. An intense band is observed in the high field region of ESR spectra. The ground state of the copper (II) complex is

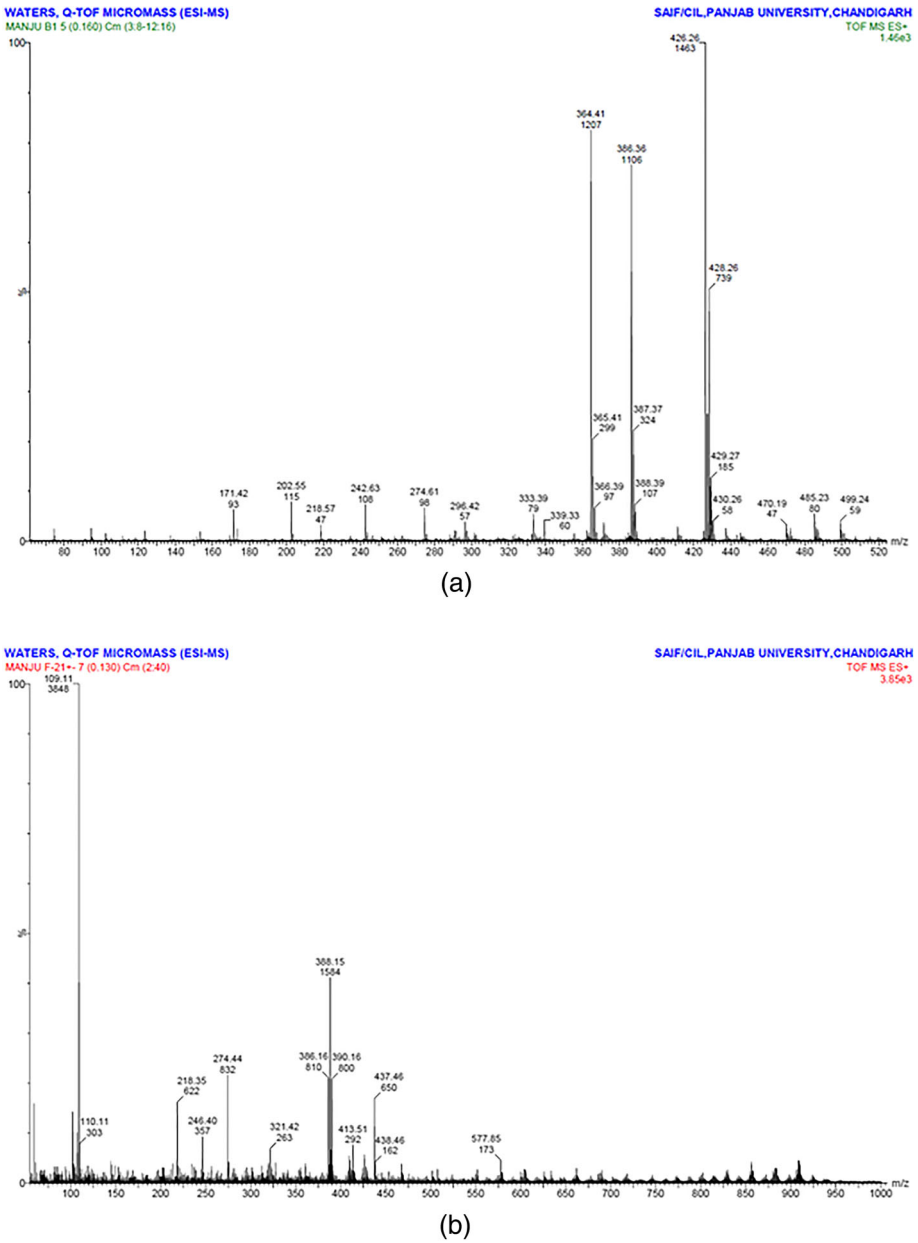

FIGURE 3 Mass spectra of (a) Schiff base 1 (b) Cobalt (II) complex (5)

acknowledged from the g tensor values, $g_{||} > g\perp > 2.0023$ which are in accordance with octahedral geometry and indicates that unpaired electron resides in the d_x^2 - $_y^2$ orbital and in the ground state as ^2B_1g.[59] The spin orbital coupling constant λ was calculated using the relation $g_{av} = 2(1- 2\lambda/10Dq)$ and g_{av} was calculated by the formulae: $1/3(g_{||} + 2\ g\perp)$ which is less than free ion Cu (II) complex, λ value (832 cm^{-1}) supported the covalent character of M–L bond in complex. Further, the observed g values for $[Cu(L_2).(CH_3COO)_2.2H_2O]$ complex were $g_{||} = 2.23$, $g\perp = 2.07$, $g_{av} = 2.12$, $G = 3.36$ were characteristic of anionic and covalent environments respectively, in metal–ligand bonding.

From the values of the g factors, geometric parameter G, representing a measure of the exchange interaction between the Cu (II) centers in polycrystalline compounds can be determined by using the following formula $G = (g_{||}\text{-}2.0023)/(g\perp - 2.0023)$.[60] If $G < 4$, it was considered the existence of some exchange interactions between the Cu (II) centers and if $G > 4$, the exchange interactions were negligible. In this complex, the G value was found to be 3.36, indicative of very little exchange interactions between the copper centers in the solid state.[61]

3.7 | X-ray diffraction spectra

The X-ray powder diffraction analysis of the compounds has been carried out in order to determine whether the

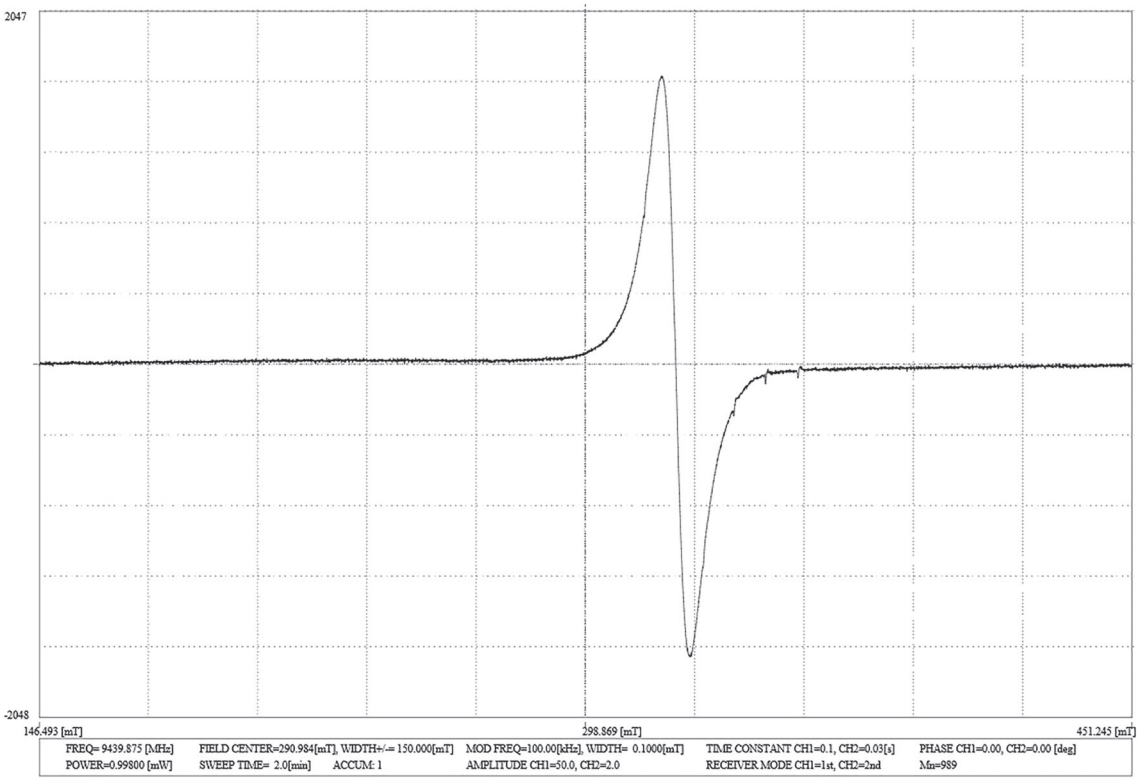

FIGURE 4 ESR spectrum of copper complex [Cu(L2).(CH3COO)2.2H2O] (11) at room temperature

nature of the sample is crystalline or amorphous and is performed by scanning the compound in the range $2\theta = 0–80°$ at a wavelength of 1.54 Å at room temperature. The powder diffraction spectra of ligand L_2 (2) and its zinc complex (12) is depicted in Figure 5. show well defined sharp peaks due to their crystalline nature. The crystallite size (D) of the compounds were calculated by using Debye Scherrer's equation:

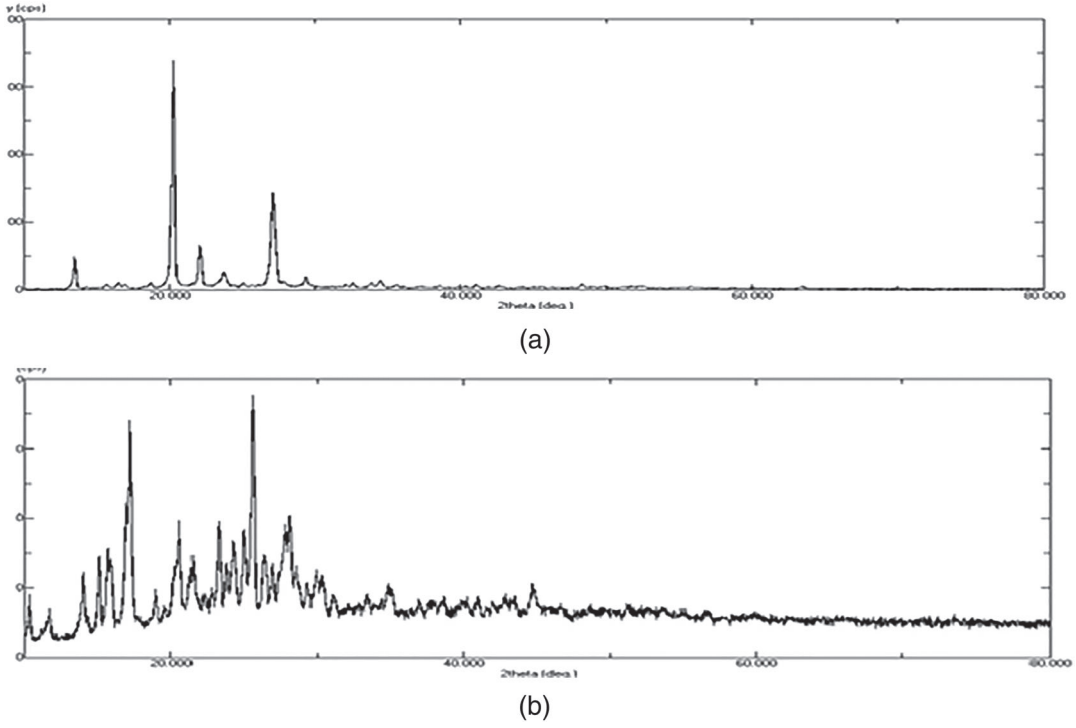

FIGURE 5 XRD Spectra of (a) Schiff base 2 (b) zinc complex 12 [Zn(L2).(CH3COO)2.2H2O]

$$\xi = \frac{0.9\lambda}{\beta\frac{1}{2}} cos\ \theta$$

where, constant 0.9 is the shape factor, λ is the X-ray wavelength of 1.5406 Å, θ is the Bragg diffraction angle and β is the full width at half maximum (FWHM). The experimental average crystallite size of ligand and its metal complex was found to be 33 and 34 nm suggesting the nanocrystalline size of the particles. The another parameter i.e. dislocation density (δ)[62,63] is the number of dislocation lines per unit area of the crystal whose value is related to the average particle diameter (D) and is calculated by the relation

$$\delta = \frac{1}{\xi^2_{XRD}}$$

The values of dislocation density (δ) was found to be in the range 0.00086–0.00092 nm^{-2}.

3.8 | Molar conductivity values

The molar conductivities of 10^{-3} M solution complexes dissolved in DMF were recorded at room temperature and the values reported in Table 1. The results obtained for the conductivity measurements of the compounds were found in the range of 11–20 $\Omega^{-1}mol^{-1}cm^2$ reveals that all the metal complexes have very low conductivity values which were characteristics for their non-electrolytic nature.[64,65]

3.9 | Thermal analysis

The thermal studies of ligands and their metal complexes were characterized within a temperature range of 25 °C to 1000 °C to elucidate the thermal stability of complexes, to decide whether the water molecules (if present) are inside or outside the coordination sphere of the central metal ion and to recommend a common scheme for thermal decomposition of these chelates. The temperature intervals and the percentage of mass loss are depicted in the graphs (Figure 6). Through IR spectral data (Table 2), it was found that two water molecules are present in the complexes; thermal analyses was carried out to ascertain their nature, and to give an insight into the thermal stability of the studied compounds. The results showed that there is a good agreement in the weight loss between the calculated and the proposed formulae. The thermal analyses imply that all complexes generally decomposed in three steps.

The DTA and TGA thermogram of $[Zn(L_2).(CH_3COO)_2.2H_2O]$ complex **(12)** showed thermal decomposition in three steps. The first peak at 180 °C with a weight loss of 6.5% (calcd. 6.3%) is assigned to elimination of two coordinated water molecules, which is accompanied by an endothermic peak. The second step appeared as an exothermic peak at 250 °C, assigned for loss of two CH_3COOH molecules with weight loss 20.4% (calcd. 20.8%). The third step appeared as an exothermic peak at 570 °C, with a weight loss of 60.9% (calcd. 61.6%) implies complete decomposition of the complex with the formation of ZnO in the end which is accompanied by an exothermic peak.

The TG and DTA thermogram of complex $[Cu(L_2).(CH_3COO)_2.2H_2O]$ **(11)** showed three decomposion steps. The first peak at 200 °C with a weight loss of 6.1% (calcd. 6.34%) represents the elimination of two coordinated water molecule, accompanied by an endothermic peak. The second step indicates weight loss of 20.2% (calcd. 20.8%) at 290 °C, assigned for the loss of two coordinating acetate molecules that is accompanied by an exothermic peak. The third step appeared as an exothermic peak near 600 °C with a weight loss of 61.1% (calcd. 61.7%) referring to the complete decomposition of this complex that ended with the formation CuO, that is accompanied by an exothermic peak.

The thermogram of the $[Co(L_2).(CH_3COO)_2.2H_2O]$ **(9)** and $[Ni(L_2).(CH_3COO)_2.2H_2O]$ **(10)** complexes also showed three steps of decomposition. The first peak appeared as an endothermic peak near 170–180 °C with a weight loss of 6.1 and 6.13% (calcd. 6.39 and 6.4%), respectively, is assigned to removal of two coordinated water molecules from each complex. The second peak appeared at 260–280 °C with a weight loss of 20.3 and 20.6% (calcd. 20.95 and 21.0%) attributed for the loss of two coordinated acetate molecules from each complex; accompanied by an exothermic peak. In the third step, an exothermic peak near 550–580 °C associated a weight loss of 61.7 and 62.6% (calcd. 62.1 and 62.2%) get appeared which was assigned for the elimination of ligand moiety from each complex, implies for complete decomposition of these complexes, respectively, ended with formation of metal oxides in the end.[66]

3.10 | Biological studies

3.10.1 | *In vitro* antibacterial activity

The antibacterial activity of synthesized compounds and the standard drug ciprofloxacin were screened against two Gram +ve bacteria (*S. aureus, S. gordonii*) and two Gram –ve bacteria (*E. coli, P. aeruginosa*). Serial dilution method was used to evaluate antibacterial activity of compounds and the data are given in Table 5 and graphical

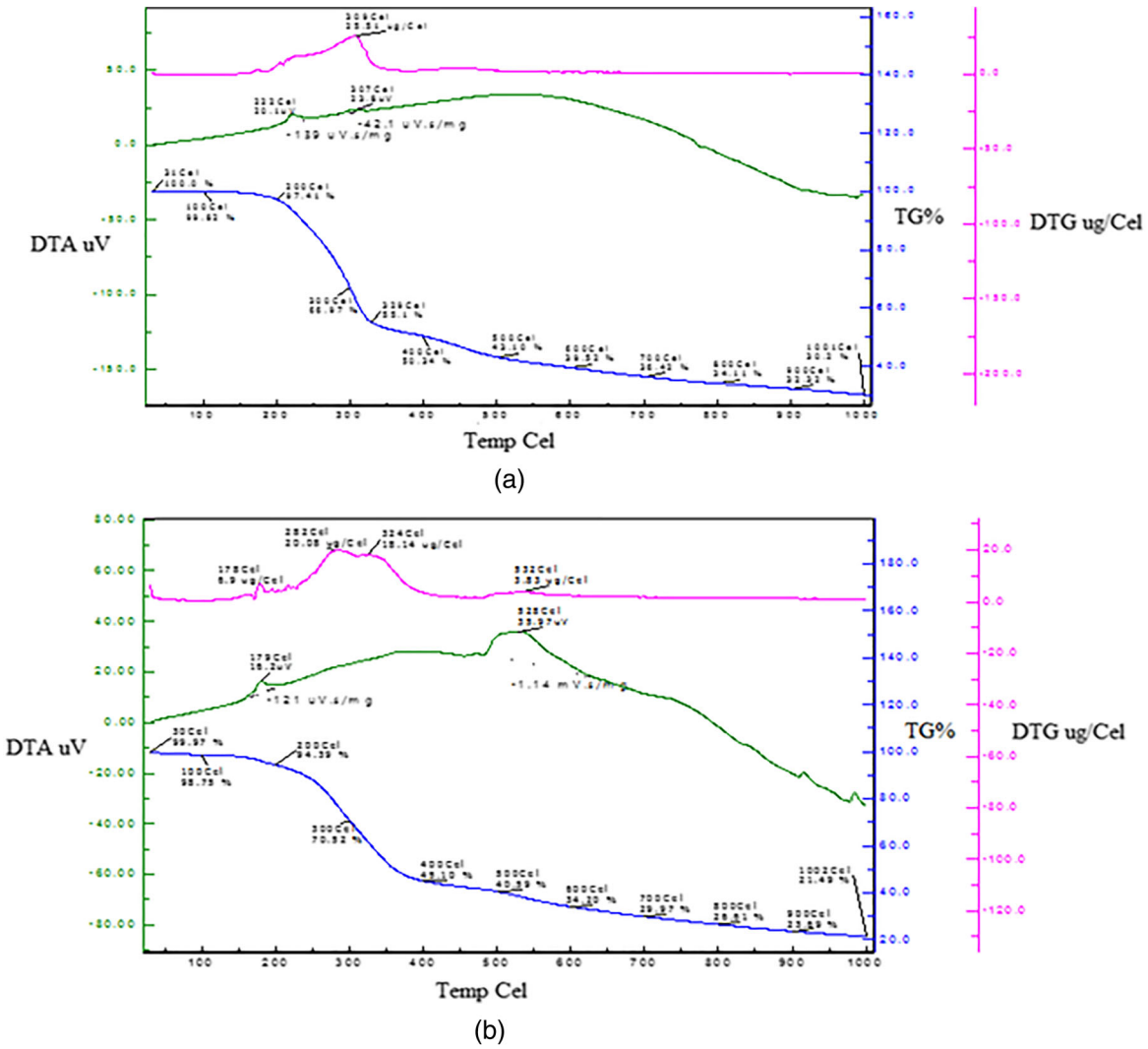

FIGURE 6 Thermogravimetric analysis plots of (a) complex 12 [Zn(L2).(CH3COO)2.2H2O] (b) complex 11 [Cu(L2).(CH3COO)2.2H2O]

representation in Figure 7. Antibacterial activity data shows that the metal complexes were more venomous than Schiff bases for the same strains under similar conditions. Metal complexes show more toxicity towards Gram +ve strains than Gram -ve strains and reason lies in the difference in the complexity of structure of the cell walls of Gram positive and Gram negative bacteria.[67]

The order of antibacterial potency for Schiff bases (L_1-L_4) was $L_4 > L_1 > L_2 > L_3$ depending on the basis of molecular weight. Further, the presence of two chloro groups in ligand L_3 makes the compound highest active.

The MIC values obtained indicate that the compounds have significantly good inhibitory effect against *S. aureus* but moderate effect against *S. gordonii* for Gram positive bacterial strains. Furthermore, the compounds **4, 9, 11, 14, 16–20** were found to be very effective against strains of *S. aureus* and complexes **11, 19** were found to be effective for *S. gordonii* species.

In case of Gram negative bacterial strains, complexes show more potency against *E. coli* as compared to *P. aeruginosa*. Compounds **5–8** and **14–20** were found to be excellent bioactive against *E. coli* strains while against *P. aeruginosa*, only complexes **16, 19** display very high activity. The variation in the antimicrobial activity of different metal complexes against different microorganisms depends on the impermeability of the cell wall or the differences in ribosomes in microbial cell. The lipid membrane surrounding the cell wall favors the passage of any lipid soluble materials and it is known that liposolubility is an important factor controlling antimicrobial activity.[68,69]

3.10.2 | *In vitro* antifungal activity

Antifungal activities of synthesized compounds were tested against two fungal strains (*C. albicans*, *A. niger*) and compared with standard antifungal drug fluconazole at the same concentration. Antifungal activity data of the compounds is summarized in Table 5 and Figure 7. The

TABLE 5 Results of *in vitro* antimicrobial screening for Schiff bases (1–4), mononuclear metal complexes (5–20) and standard drugs (21, 22). (MIC in μM/ml)

		Gram +ve bacteria		Gram –ve bacteria		Fungus	
S. No.	Compounds	S. aureus	S. gordonii	E.coli	P. aeruginosa	C. albicans	A. niger
1	L_1	0.0343	0.0343	0.0343	0.0343	0.0343	0.0343
2	L_2	0.0358	0.0358	0.0358	0.0358	0.0358	0.0358
3	L_3	0.0253	0.0506	0.0506	0.0506	0.0253	0.0506
4	L_4	0.0170	0.0340	0.0340	0.0340	0.0170	0.0340
5	$Co(L_1).(CH_3COO)_2.2H_2O$	0.0217	0.0217	0.0108	0.0217	0.0217	0.0217
6	$Ni(L_1).(CH_3COO)_2.2H_2O$	0.0217	0.0217	0.0109	0.0217	0.0217	0.0217
7	$Cu(L_1).(CH_3COO)_2.2H_2O$	0.0215	0.0215	0.0108	0.0215	0.0108	0.0215
8	$Zn(L_1).(CH_3COO)_2.2H_2O$	0.0215	0.0215	0.0107	0.0215	0.0107	0.0215
9	$Co(L_2).(CH_3COO)_2.2H_2O$	0.0111	0.0222	0.0222	0.0222	0.0111	0.0222
10	$Ni(L_2).(CH_3COO)_2.2H_2O$	0.0222	0.0223	0.0223	0.0221	0.0111	0.0223
11	$Cu(L_2).(CH_3COO)_2.2H_2O$	0.0110	0.0110	0.0221	0.0221	0.0110	0.0221
12	$Zn(L_2).(CH_3COO)_2.2H_2O$	0.0220	0.0220	0.0220	0.0220	0.0110	0.0220
13	$Co(L_3).(CH_3COO)_2.2H_2O$	0.0272	0.0271	0.0272	0.0272	0.0136	0.0272
14	$Ni(L_3).(CH_3COO)_2.2H_2O$	0.0136	0.0272	0.0136	0.0272	0.0136	0.0272
15	$Cu(L_3).(CH_3COO)_2.2H_2O$	0.0269	0.0269	0.0135	0.0269	0.0135	0.0269
16	$Zn(L_3).(CH_3COO)_2.2H_2O$	0.0134	0.0269	0.0134	0.0134	0.0134	0.0134
17	$Co(L_4).(CH_3COO)_2.2H_2O$	0.0108	0.0215	0.0108	0.0215	0.0108	0.0215
18	$Ni(L_4).(CH_3COO)_2.2H_2O$	0.0108	0.0216	0.0108	0.0216	0.0108	0.0216
19	$Cu(L_4).(CH_3COO)_2.2H_2O$	0.0107	0.0107	0.0107	0.0107	0.0107	0.0107
20	$Zn(L_4).(CH_3COO)_2.2H_2O$	0.0109	0.0214	0.0107	0.0214	0.0214	0.0107
21	Ciprofloxacin	0.0047	0.0047	0.0047	0.0047	-	-
22	Fluconazole	-	-	-	-	0.0051	0.0102

metal complexes were more potent fungicides than the respective Schiff bases and activity further got enhanced at higher concentrations. DMSO control has shown a negligible activity as compared to the metal complexes and Schiff bases.

The trend of potency followed by Schiff base ligands (L_1-L_4) against fungal strains was also found to be $L_4 > L_1 > L_2 > L_3$ as explained earlier for antibacterial activity. All the metal complexes exhibit more potency against *C. albicans* than *A. niger*. Against *A. niger*, complexes **16, 19** and **20** were found to be excellent effective with MIC values 0.0134 and 0.0107 μM/mL equivalent with that of standard drug (MIC = 0.0102 μM/ml). Compounds **5–15** and **18** were also found to be good antifungal agent against *A. niger* with nearly half potency than the standard.

Against *C. albicans*, the complexes **7–19** showed high antifungal activity; almost half potency with MIC values in the range 0.010 to 0.013 μM/ml than fluconazole (MIC = 0.0051 μM/mL). The trend of fungal growth inhibition in the complexes was found to be in the order Zn (II) > Cu (II) > Co (II) > Ni (II). The low activity of some metal complexes may be due to their low lipophilicity, because of which penetration of the complex through the lipid membrane was decreased and hence, they could neither block nor inhibit the growth of the microorganism.[68]

On conclusion, we can assert that copper complex **16** was the potent antimicrobial agent, while zinc complex **19** was the highest potent antimicrobial compound in the series studied. While considering the overall order, it was found that zinc complexes were the highest noxious compounds among all the synthesized compounds against all microbial strains.

The antimicrobial activity of synthesized Schiff bases may be due to the existence of the (-C=N-) moiety which have chelating properties. The mode of action of these compounds may involve the construction of hydrogen bond through azomethine/carbonyl group with the active centers of the cell constituents, resulting in obstruction in

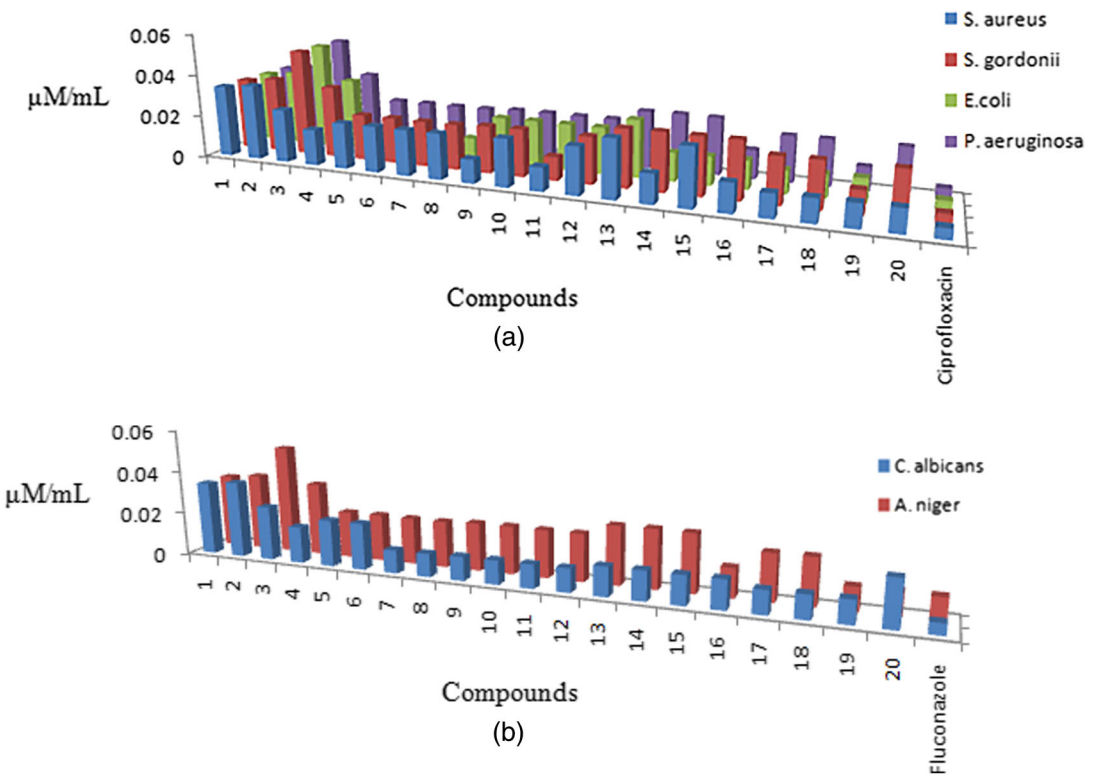

FIGURE 7 Graphical representation of (a) Antibacterial activity (b) antifungal activity of Schiff base ligands and their complexes

normal life cell processes. The biological data divulges that the coordination of Schiff bases to metal ions leads to amplification in antimicrobial activity of complexes than the free parent Schiff bases. The enhanced activity of these metal complexes may be due to presence of an additional factor of chelation through imine bond (-C=N-) which certifies the increased lipophilic nature of complexes.[69] On chelation, the polarity of the metal ion will be reduced to a greater extent due to overlapping of the ligand orbitals and partial sharing of the positive charge of the metal ion with ligand donor groups. Further, it increases the delocalization of p-electrons over the whole chelated ring and enhances the penetration of the complexes into lipid membranes and blocking the metal binding sites in enzymes of microorganism.[70] These complexes also perturb the respiration process of the cells and thus, blocks the synthesis of proteins, which restricts further growth of microorganisms.[71] It was also noted that the toxicity of the metal chelates increases on increasing the concentration of metal ions, probably owing to faster diffusion of these chelates as a whole via cell membrane due to which further development of organisms get caught up.

Apart from above considerations, the antimicrobial activity of compounds also depends on the nature of the ligands, their concentration, nature of metal ion, nature of anions surrounding the metal ion, number and nature of coordinating sites and geometry of complexes.

3.11 | Anticancer activity

To evaluate the potential of the synthesized compounds for growth inhibition of cancerous cells, the synthesized compounds were screened *in vitro* against following malignant tumor cell lines namely, human alveolar adenocarcinoma epithelial cell line (A549), human breast adenocarcinoma cell line (MCF7), human prostate cancer cell line (DU145) and human normal lung cell line (MRC5) using MTT assay and compared with the standard reference drug (doxorubicin). Accessed cytotoxicity of all the test compounds was expressed as IC_{50} value (i.e. the concentration which inhibits 50% growth) obtained after exposure to 48 hours against four cell lines and values summarized in Table 6 and Figure 8.

The synthesized Schiff base ligands and their complexes having different substituents were tested for anticancer activities and the calculated IC_{50} values demonstrated that compound **(16)** $[Zn(L_3)(CH_3COO)_2.2H_2O]$ displayed highest activity among all the synthesized compounds with an IC_{50} values of 10.6, 13.4 and 12.9 µM against A549, MCF7 and DU145 cancer cell lines, respectively. Further, **(8)** and **(12)** zinc complexes also showed very fine activity having IC_{50} value <20 μM, while the compounds **(1)**, **(2)**, **(3)**, **(5)**, **(6)**, **(7)**, **(9)**, **(10)**, **(11)**, **(13)**, **(14)** and **(15)** showed moderate anticancer activity against A549, MCF7 and DU145 cell lines. Moreover, the compounds **(19)** and **(20)** were found to be

TABLE 6 Cytotoxicity of Schiff bases and their respective complexes using three cancer cell lines (A549, MCF7, DU145) and one normal cell line (MRC-5) after revelation for 48 hrs

		IC_{50} values (μM ± S.D.)[a]			
Sr. No.	Test compound	A549	MCF7	DU145	MRC5
1	L_1	20.5 ± 0.19	25.6 ± 0.50	30.4 ± 0.26	96.9 ± 0.22
2	L_2	24.2 ± 0.25	27.1 ± 0.38	25.4 ± 0.61	89.4 ± 0.25
3	L_3	20.3 ± 0.28	18.5 ± 0.43	21.9 ± 0.12	94.2 ± 0.67
4	L_4	11.2 ± 0.44	14.7 ± 0.68	15.2 ± 0.21	80.0 ± 0.37
5	$Co(L_1).(CH_3COO)_2.2H_2O$	27.7 ± 0.18	26.8 ± 0.20	25.2 ± 0.17	97.1 ± 0.27
6	$Ni(L_1).(CH_3COO)_2.2H_2O$	19.6 ± 0.22	22.1 ± 0.24	21.5 ± 0.63	92.1 ± 0.71
7	$Cu(L_1).(CH_3COO)_2.2H_2O$	21.4 ± 0.33	19.3 ± 0.25	23.2 ± 0.19	84.1 ± 0.55
8	$Zn(L_1).(CH_3COO)_2.2H_2O$	16.6 ± 0.22	17.8 ± 0.32	19.8 ± 0.35	102.1 ± 0.43
9	$Co(L_2).(CH_3COO)_2.2H_2O$	26.1 ± 0.34	29.3 ± 0.54	25.9 ± 0.43	95.3 ± 0.61
10	$Ni(L_2).(CH_3COO)_2.2H_2O$	20.9 ± 0.22	23.7 ± 0.42	22.5 ± 0.64	90.0 ± 0.51
11	$Cu(L_2).(CH_3COO)_2.2H_2O$	21.0 ± 0.50	22.4 ± 0.37	26.3 ± 0.10	80.2 ± 0.42
12	$Zn(L_2).(CH_3COO)_2.2H_2O$	16.8 ± 0.21	20.0 ± 0.23	18.2 ± 0.24	101.6 ± 0.52
13	$Co(L_3).(CH_3COO)_2.2H_2O$	25.1 ± 0.32	21.8 ± 0.41	24.1 ± 0.52	90.2 ± 0.13
14	$Ni(L_3).(CH_3COO)_2.2H_2O$	17.4 ± 0.12	16.5 ± 0.59	20.7 ± 0.44	98.3 ± 0.67
15	$Cu(L_3).(CH_3COO)_2.2H_2O$	18.8 ± 0.24	17.0 ± 0.45	20.8 ± 0.48	109.2 ± 0.53
16	$Zn(L_3).(CH_3COO)_2.2H_2O$	10.6 ± 0.14	13.4 ± 0.38	12.9 ± 0.53	93.9 ± 0.56
17	$Co(L_4).(CH_3COO)_2.2H_2O$	-	-	57.4 ± 0.12	-
18	$Ni(L_4).(CH_3COO)_2.2H_2O$	-	-	-	-
19	$Cu(L_4).(CH_3COO)_2.2H_2O$	43.2 ± 0.67	39.2 ± 0.86	48.3 ± 0.68	98.0 ± 0.27
20	$Zn(L_4).(CH_3COO)_2.2H_2O$	34.6 ± 0.19	45.4 ± 0.11	58.0 ± 0.23	87.2 ± 0.54
Std	Doxorubicin	0.7 ± 0.11	0.9 ± 0.08	0.8 ± 0.06	10.2 ± 0.18

Not active

A549- Human lung carcinoma cell line

MCF7- Human breast carcinoma cell line

DU145- Human prostate carcinoma cell line

MRC5- Normal human lung cell line

[a](IC_{50}) = concentration of drug required to inhibit growth of 50% of tumor cells. The data are mean ± standard deviation and represents the average of three sets of independent trials.

least potent with high IC_{50} values and compound **(17)** was found inactive against all cancer cell lines except DU145 with low potency. Further, the compound **(18)** was found to be inactive against all the tested cell lines.

It was found that the Schiff base ligand L_4 **(4)** was found to be highest active with IC_{50} values 11.2, 14.7 and 15.2 μM against A549, MCF7 and DU145 cancer cell lines, respectively (owing to two chloro group present on benzene ring) and ligand L_2 **(2)** is least active against A549 and MCF7 while ligand L_1 **(1)** is least active against DU145 cell line. Further, the conclusions obtained from the anticancer data revealed that complexes **(5–8)** of ligand L_1 **(1)** were found to be active against all the three cancer cell lines due to the presence of aromatic planar ring system and hydrophobic nature but its zinc complex was found to be highly potent among its all the four complexes followed by nickel and copper complexes. Similarly, the zinc complex of ligand L_2 was found to be highest active against all tested strains followed by nickel, copper and cobalt. These outcomes are expected as there is difference of a single methylene group in the structures of ligand L_1 **(1)** and L_2 **(2)**. Further, zinc complex **(16)** of ligand L_3 **(3)** was the highest active amongst the entire synthesized compounds against all the cancer cell lines followed by the same pattern as discussed above which may be attributed by the presence of the acetylenic group in the structure. Further, the zinc and copper complexes of ligand L_4 **(4)** were somewhat active against all cell lines, cobalt complex was active against only DU145 cell line and nickel complex was found to be inactive against

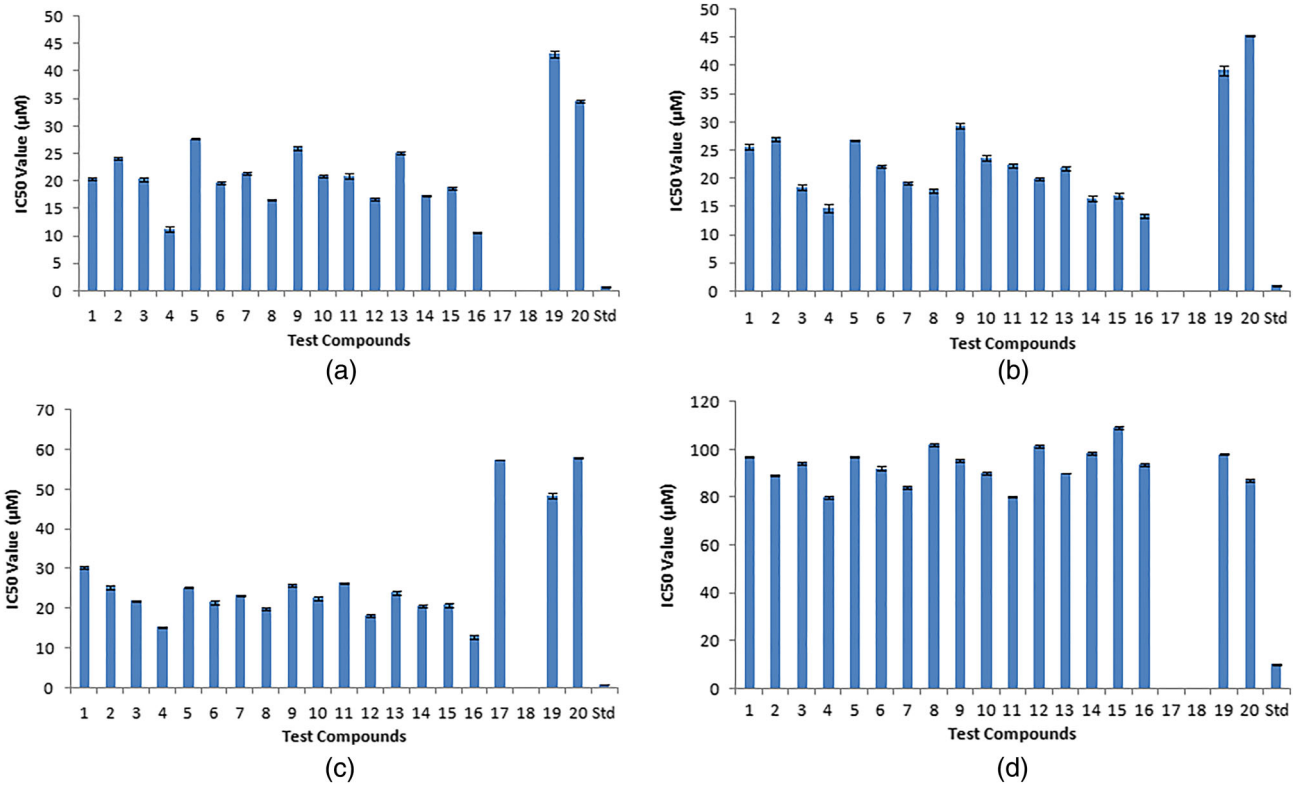

FIGURE 8 Anticancer activities of Schiff bases and their transition metal complexes against (a) Human lung carcinoma cell line (A549), (b) Human breast carcinoma cell line (MCF7), (c) Human prostate carcinoma cell line (DU145) and (d) Normal human lung cell line (MRC-5)

all the cancer cell lines. The concluded trend of potency followed by transition metal complexes **(1–20)** against three cancer cell lines was found to be Zn > Ni > Cu > Co.

Furthermore, the evaluation against human normal cell line (MRC5), demonstrated that the compounds were 8–11 times less toxic as compared with the standard drug doxorubicin,[72] except complexes **(17)** and **(18)** which did not induce any toxicity against the normal cell line which may be a buoyant and optimistic dot for the present research work. But on the other hand they were also found to be inactive against cancer cell lines. The other important aspect for toxicity was that the compound **(15)** (IC_{50} value 109.2) was found to be almost 11 folds less toxic than the standard drug doxorubicin (IC_{50} value 10.2) which along with its moderate activity, makes this compound most appealing candidate among the entire synthesized compounds for the curative purpose of cancer. Similarly, the complex **(16)** along with its uppermost cytotoxicity in opposition to malignant cell lines was found as 9 times least toxic than the standard drug for normal human cell line and might be measured as the compound of paramount importance amongst the present tested compounds.

The cytotoxicity of compounds is dependent on their ability to bind with DNA and subsequent impairment of its structure and functions followed by interference in replication and transcription process ultimately leading to cell death.[73,74] Apart from this, the positive charge of the metal increases the acidity of coordinated ligands causing stronger hydrogen bonding resulting in enhanced cytotoxic activity. The variation in substituents and the metal ions clearly affects the binding ability to DNA and corresponding alteration in biological activity is observed in the present case also. Further, it was concluded that electron-withdrawing chloro groups on aryl ring contributed significantly towards cytotoxic potential of ligand $\mathbf{L_4}$ against all the three cancer cell lines, but the effect of the acetylinic group is even more pronounced as is evident from the activity of compound **(16)** zinc complex of ligand $\mathbf{L_3}$.

4 | CONCLUSIONS

In the current study of research, our booming efforts are the synthesis of some novel mononuclear Schiff base complexes of Co (II), Ni (II), Cu (II) and Zn (II). The Schiff bases were obtained from condensation of substituted napthaldehyde/benzaldehyde/salicylaldehyde derivatives with 4-methyl-3-thiosemicarbazide and were further reacted by corresponding metal (II) acetates to form complexes in 1:1 molar ratio. A comparative physicochemical and spectral study of synthesized compounds has been

done which provides excellent data and is in good agreement with the proposed octahedral structure. The spectral data studies revealed that Schiff bases coordinates in a bidentate manner via nitrogen atom of azomethine group and sulfur atom of thione group and does not exists in thio-enol tautomerism during complexation. The XRD patterns designate the crystalline nature of complexes. *In vitro* antimicrobial studies demonstrate enhancement in metal complexes potency on complexation than parent Schiff bases and zinc complexes were found as the most potent. In addition to this, compounds were also evaluated for cytotoxicity against three cancer cell lines and one normal human cell line which displayed moderate to good inhibitory activities and revealed that complex **(16)** $[Zn(L_3)(CH_3COO)_2.2H_2O]$ displayed the highest cytotoxicity amongst all compounds with an IC_{50} values of 10.6, 13.4 and 12.9 μM against A549, MCF7 and DU145 cancer cell lines, respectively that might turn out to be high-quality anticancer mediator in medical trials. The compound **(15)** and **(16)** (IC_{50} value 109.2 and 90.5) was found to be almost 11 and 9 times less toxic than the standard drug doxorubicin (IC_{50} value 10.2) against normal cell line MRC5 and good toxic agents against cancer cell lines which acts as expectant treatment for the cancer by means of slightest destructive possessions in organization of patients body parts. The highest potency of zinc complexes against all the above tested strains suggests analogous relation between cytotoxicity and antimicrobial screening. Thus, the study in the present manuscript deals with new valuable insights for scheming various metallopharmaceuticals for anticancer therapy.

ACKNOWLEDGMENTS

The author Ms. Manju Yadav (SRF) thanks to University Grant Commission, New Delhi, India for the award of JRF-SRF Fellowship with reference no. 23/06/2013(i) EU-V dated 23/12/2013, Dr. A.P.J. Abdul Kalam central instrumentation laboratory and Department of Chemistry of Guru Rameshwar University of Science & Technology, Hisar for providing facilities to carry out this research work.

ORCID

J. Devi https://orcid.org/0000-0003-0434-3193

REFERENCES

[1] C. Elamathi, R. Butcher, R. Prabhakaran, *Appl. Organomet. Chem.* **2018**, *32*, 4364.

[2] W. C. Huang, Y. J. Chen, M. C. Hung, *Biomedica* **2011**, *1*, 2.

[3] A. Persidis, *Nat. Biotechnol.* **1999**, *17*, 94.

[4] E. Wong, C. M. Giandomenico, *Chem. Rev.* **1999**, *99*, 2451.

[5] A. M. Angeles-Boza, P. M. Bradley, P. K. L. Fu, S. E. Wicke, J. Bacsa, K. M. Dunbar, C. Turro, *Inorg. Chem.* **2004**, *43*, 8510.

[6] L. Viganor, O. Howe, P. McCarron, M. McCann, M. Devereux, *Curr. Top. Med. Chem.* **2017**, *17*, 1280.

[7] M. Wehbe, A. W. Leung, M. J. Abrams, C. Orvig, M. B. Bally, *Dalton Trans.* **2017**, *46*, 10758.

[8] N. C. Saha, R. J. Butcher, S. Chaudhuri, N. Saha, *Polyhedron* **2003**, *22*, 383.

[9] V. B. Arion, M. A. Jakupec, M. Galanski, P. Unfried, B. K. Keppler, *J. Inorg. Biochem.* **2002**, *91*, 298.

[10] D. R. Richardson, P. V. Bernhardt, *J. Biol. Inorg. Chem.* **1999**, *4*, 266.

[11] L. H. Abdel-Rahman, A. M. Abu-Dief, S. K. Hamdan, A. A. Seleem, *Int. J. Nano. Chem.* **2015**, *1*, 65.

[12] L. H. Abdel-Rahman, A. M. Abu-Dief, E. F. Newair, S. K. Hamdan, *J. Photochem. Photobiol. B* **2016**, *160*, 18.

[13] J. S. Casas, M. S. Garcia-Tasende, J. Sordo, *J. Coord. Chem. Rev.* **2000**, *209*, 197.

[14] D. Mishra, S. Naskar, M. G. B. Drew, S. K. Chattopadhyay, *Inorg. Chim. Acta* **2000**, *359*, 585.

[15] R. R. Crichton, D. T. Dexter, R. J. Ward, *Coord. Chem. Rev.* **2008**, *252*, 1189.

[16] A. Chakraborty, P. Kumar, K. Ghosh, P. Roy, *Eur. J. Pharmacol.* **2010**, *647*, 1.

[17] M. Wang, L. F. Wang, Y. Z. Li, Q. X. Li, Z. D. Xu, D. M. Qu, *Transition Met. Chem.* **2001**, *26*, 307.

[18] H. L. Singh, *Spectrochim. Acta A* **2010**, *76*, 253.

[19] N. Dharamraj, P. Viswanathanmurthi, K. Natarajan, *Transition Met. Chem.* **2001**, *26*, 105.

[20] K. M. Khan, A. Ahmad, N. Ambreen, A. Amyn, S. Perveen, S. A. Khan, M. I. Choudhary, *Lett. Drug. Des. Discov.* **2009**, *6*, 363.

[21] K. M. Khan, N. Ambreen, U. R. Mughal, S. Jalil, S. Perveen, M. I. Choudhary, *Eur. J. Med. Chem.* **2010**, *45*, 4058.

[22] F. Zhao, W. Wang, W. Lu, L. Xub, S. Yang, X. Cai, M. Zhou, M. Lei, M. Ma, H. Xu, F. Cao, *Eur. J. Med. Chem.* **2018**, *146*, 451.

[23] S. G. Kucukguzel, S. Rollas, I. Kuukguzel, M. Kiraz, *Eur. J. Med. Chem.* **1999**, *34*, 1093.

[24] S. Zhang, A. D. Sherry, *J. Solid State Chem.* **2003**, *171*, 38. I. P. Ejidike, P. A. Ajibade, *Bioinorg. Chem. Appl.* **2015**, *2015*, 1.

[25] H. F. A. El-Halim, G. G. Mohamed, M. N. Anwar, *Appl. Organomet. Chem.* **2017**, *32*, 3899.

[26] B. Annaraj, C. Balakrishnan, M. A. Neelakantan, *J. Photochem. Photobiol. B* **2016**, *160*, 278.

[27] B. M. Mistry, S. Jauhari, *Res. Chem. Intermed.* **2013**, *39*, 1049.

[28] P. P. Sarmah, B. Deb, B. J. Borah, A. L. Fuller, A. M. Z. Slawin, J. D. Woollins, D. K. Dutta, *J. Organomet. Chem.* **2010**, *695*, 2603.

[29] S. Ramakrishnan, D. Shakthipriya, E. Suresh, V. S. Periasamy, M. A. Akbarsha, M. Palaniandavar, *Inorg. Chem.* **2011**, *50*, 6458.

[30] K. Lal, P. Yadav, A. Kumar, *Med. Chem. Res.* **2016**, *25*, 644.

[31] H. F. A. El-Halim, M. M. Omar, M. N. Anwar, *J. Therm. Anal. Calorim.* **2017**, *130*, 1069.

[32] T. Mosmann, *J. Immunol. Methods* **1983**, *65*, 55.

[33] H. F. A. El-Halim, G. G. Mohamed, M. N. Anwar, *Appl. Organomet. Chem.* **2018**, *32*, 3899.

[34] A. A. A. Aziz, I. S. A. El-Sayed, M. M. H. Khalil, *Appl. Organomet. Chem.* **2017**, *31*, 3730.

[35] C. Anitha, C. D. Sheela, P. Tharmaraj, S. J. Raja, *Spectrochim. Acta A* **2012**, *98*, 35.

[36] A. J. M. Al-Karawi, A. A. A. Al-Dulimi, A. M. A. A. Al-Mokaram, *Saudi Arabia.* **2012**, *24*, 25.

[37] D. X. West, A. A. Nassar, F. A. El-Saied, M. I. Ayad, *Transition Met. Chem.* **1998**, *23*, 423.

[38] P. M. Krishna, B. S. Shankara, N. S. Reddy, *Int. J. Inorg. Chem.* **2013**, *2013*, 1.

[39] W. H. Mahmoud, R. G. Deghadi, G. G. Mohamed, *Appl. Organomet. Chem.* **2016**, *30*, 221.

[40] W. H. Mahmoud, R. G. Deghadi, G. G. Mohamed, *J. Therm. Anal. Calorim.* **2017**, *127*, 2149.

[41] K. Nakamoto, *Infrared spectra of inorganic and coordination compounds*, John Wiley and Sons, New York **1996**.

[42] R. El-Shazly, G. El-Hazmi, S. Ghazy, M. El-Shahawi, A. El-Asmy, *Spectrochim. Acta A* **2005**, *61*, 243.

[43] F. A. El-Saied, A. A. El-Asmy, W. Kaminsky, D. X. West, *Transition Met. Chem.* **2003**, *28*, 954.

[44] K. Singh, Y. Kumar, P. Puri, C. Sharma, K. R. Aneja, *Bioinorg. Chem. Appl.* **2011**, *2011*, 1.

[45] L. N. Suvarapu, S. O. Baek, *Metals.* **2015**, *5*, 2266.

[46] M. M. Hassanien, I. M. Gabr, M. H. Abdel-Rhman, A. A. El-Asmy, *Spectrochim. Acta A* **2008**, *71*, 73.

[47] A. J. M. Al-Karawi, *Transition Met. Chem.* **2009**, *34*, 891.

[48] L. Rejani, M. T. Leticia, M. Tania, B. Heloisa, *J. Braz. Chem. Soc.* **1999**, *10*, 184.

[49] E. N. M. Yusof, T. B. S. Ravoof, E. R. T. Tiekink, A. Veerakumarasivam, K. A. Crouse, M. I. M. Tahir, H. Ahmad, *Int. J. Mol. Sci.* **2015**, *16*, 11034.

[50] I. Dilovic, M. Rubcic, V. Vrdoljak, S. K. Pavelic, M. Kralj, I. Piantanida, M. Cindric, *Bioorg. Med. Chem.* **2008**, *16*, 5189.

[51] T. B. Demirci, M. Şahin, E. Kondakci, M. Ozyurek, B. Ulkuseven, R. Apak, *Spectrochim. Acta A* **2015**, *138*, 866.

[52] S. A. A. El-Enein, F. A. El-Saied, T. I. Kasher, A. H. El-Wardany, *Spectrochim. Acta A* **2007**, *67*, 737.

[53] P. A. Ajibade, G. A. Kolawole, P. O'Brien, M. Helliwell, J. Raftery, *Inorg. Chim. Acta* **2006**, *359*, 3111.

[54] G. G. Mohammed, *Spectrochim. Acta A* **2001**, *57*, 1643.

[55] J. C. Bailar, H. J. Emeleus, R. Nyholm, A. F. T. Dickenson, *Comprehensive inorganic chemistry*, Pergamon, Oxford **1975**.

[56] R. A. Ammar, A. M. A. Alaghaz, A. S. Alturiqi, *Appl. Organomet. Chem.* **2018**, *32*, 4361.

[57] A. M. A. Alaghaz, R. A. Ammar, *Eur. J. Med. Chem.* **2010**, *45*, 1314.

[58] J. Devi, M. Yadav, A. Kumar, A. Kumar, *Chem. Pap.* **2018**, *72*, 2479.

[59] W. H. Mahmoud, G. G. Mohamed, O. Y. El-Sayed, *Appl. Organomet. Chem.* **2017**, *32*, 4051.

[60] P. Tyagi, M. Tyagi, S. Agrawal, S. Chandra, H. Ojha, M. Pathakd, *Spectrochim. Acta A* **2017**, *171*, 246.

[61] M. A. Diab, A. Z. El-Sonbati, A. A. El-Bindary, G. G. Mohamed, S. M. Morgan, *Res. Chem. Intermed.* **2015**, *41*, 9029.

[62] P. P. Utthra, G. Kumaravel, R. Senthilkumar, N. Raman, *Appl. Organomet. Chem.* **2017**, *31*, 3629.

[63] S. Velumani, X. Mathew, P. J. Sebastian, S. K. Narayandass, D. Mangalaraj, *Sol. Energy Mater sol. Cell* **2003**, *76*, 347.

[64] W. J. Geary, *Coord. Chem. Rev.* **1971**, *7*, 81.

[65] A. N. Srivastva, N. P. Singh, C. K. Shriwastaw, *Arab. J. Chem.* **2016**, *9*, 48.

[66] A. S. El-Tabl, M. M. A. El-Waheed, M. A. Wahba, N. A. El-Halim Abou El-Fadl, *Bioinorg. Chem. Appl.* **2015**, *2015*, 1.

[67] J. Devi, N. Batra, *Spectrochim. Acta A* **2015**, *135*, 710.

[68] N. Dharmaraj, P. Viswanathamurthi, K. Natarajan, *Transition Met. Chem.* **2002**, *26*, 105.

[69] J. Devi, N. Batra, R. Malhotra, *Spectrochim. Acta A* **2012**, *97*, 397.

[70] E. Ispir, *Dyes Pigm.* **2009**, *82*, 13.

[71] R. S. Joseyphus, M. S. Nair, *Mycobiology.* **2008**, *36*, 93.

[72] J. D. Chellaian, J. Johnson, *Spectrochim. Acta A* **2014**, *127*, 396.

[73] A. Caudhary, R. V. Singh, *Phosphorus, Sulfur Silicon Relat. Elem.* **2003**, *178*, 603.

[74] J. Devi, M. Yadav, D. Kumar, L. S. Naik, D. K. Jindal, *Appl. Organomet. Chem.* **2019**, *33*, 4693.

SUPPORTING INFORMATION

Additional supporting information may be found online in the Supporting Information section at the end of the article.

How to cite this article: Devi J, Yadav M, Jindal DK, Kumar D, Poornachandra Y. Synthesis, spectroscopic characterization, biological screening and *in vitro* cytotoxic studies of 4-methyl-3-thiosemicarbazone derived Schiff bases and their Co (II), Ni (II), Cu (II) and Zn (II) complexes. *Appl Organometal Chem*. 2019;e5154. https://doi.org/10.1002/aoc.5154